P-06-141

# Forsmark site investigation

# Groundwater flow measurements and SWIW test in borehole KFM04A

Erik Gustafsson, Rune Nordqvist, Pernilla Thur
Geosigma AB

November 2006

**Svensk Kärnbränslehantering AB**
Swedish Nuclear Fuel
and Waste Management Co
Box 5864
SE-102 40 Stockholm Sweden
Tel 08-459 84 00
+46 8 459 84 00
Fax 08-661 57 19
+46 8 661 57 19

ISSN 1651-4416
SKB P-06-141

# Forsmark site investigation

# Groundwater flow measurements and SWIW test in borehole KFM04A

Erik Gustafsson, Rune Nordqvist, Pernilla Thur
Geosigma AB

November 2006

*Keywords:* PF 400-06-002, Forsmark, Hydrogeology, Borehole, Groundwater, Flow, Tracer tests, Dilution probe, SWIW test.

# Abstract

This report describes the performance, evaluation and interpretation of in situ groundwater flow measurements and a single well injection withdrawal tracer test (SWIW test) at the Forsmark site. The objectives of the activity were to determine the natural groundwater flow in selected fractures/fracture zones intersecting the core drilled borehole KFM04A, as well as to determine transport properties of fractures by means of a SWIW test in the borehole.

Groundwater flow measurements were carried out in two single fractures and in two fracture zones at borehole lengths ranging from c. 232 to c. 422 m (204 to 365 m vertical depth). The hydraulic transmissivity ranged within $T = 8.9 \cdot 10^{-9}$–$5.5 \cdot 10^{-5}$ $m^2/s$. The results of the dilution measurements in borehole KFM04A show that the groundwater flow varies considerably in fractures and fracture zones during natural, i.e. undisturbed, conditions. Nevertheless the general trend is that flow rates and Darcy velocities decrease with depth. The flow rate ranged from 0.004 to 16.6 ml/min and the Darcy velocity from $3.5 \cdot 10^{-10}$ to $3.6 \cdot 10^{-7}$ m/s ($3.0 \cdot 10^{-5}$–$3.1 \cdot 10^{-2}$ m/d), results which are in accordance with results from previously performed dilution measurements under natural gradient conditions at the Forsmark site. The highest single flow rate and Darcy velocity were measured in the section with several flowing fractures in the upper part of deformation zone ZFMNE00A2. Hydraulic gradients, calculated according to the Darcy concept, are within the expected range (0.001–0.05) in two of four measured sections. The determined groundwater flow rates are fairly proportional to the hydraulic transmissivity although the statistical basis is weak.

Measurements were also attempted in two low transmissive ($T < 10^{-9}$ $m^2/s$) sections at c. 517 m and c. 522 m borehole length (442 and 446 m vertical depth). Unfortunately, the measurements had to be stopped due to technical problems in combination with high density of particles and a chemical composition in the borehole water causing drift in the optical device.

The SWIW test was carried out in the upper part of deformation zone ZFMNE1188 at a borehole length of c. 417 m (361 m vertical depth) with a hydraulic transmissivity of $T = 8.9 \cdot 10^{-9}$ $m^2/s$.

Several anomalous features of the experimental data made it difficult to perform a quantitative interpretation normally carried out using a radial flow model with advection, dispersion and linear equilibrium sorption as transport processes, of the results. Tracer recovery was only 42.6%, 53.9% and 32.8% for Uranine, rubidium and cesium, respectively. Although the test was stopped before the tracer breakthrough had returned to background values, plausible extrapolations of the recovery curve still indicate that significant loss of tracer is likely to have occurred, possibly caused by tracer being pushed out to other fractures or fracture zones with higher natural flow. Further, the breakthrough curve for cesium gives an ambiguous impression as it indicates a very weak retention in the early parts but much stronger retention in the later parts. For this reason, no estimate of a retardation factor for cesium is presented. Estimates of the retardation factor for rubidium ranged from 2.9 to 5.5. However, these values should be considered as very uncertain.

# Sammanfattning

Denna rapport beskriver genomförandet, utvärderingen samt tolkningen av in situ grundvattenflödesmätningar och ett enhålsspårförsök (SWIW test) i Forsmark. Syftet med aktiviteten var dels att bestämma det naturliga grundvattenflödet i enskilda sprickor och sprickzoner som skär borrhålet KFM04A, dels att karaktärisera transportegenskaperna i potentiella flödesvägar genom att utföra och utvärdera ett SWIW test i borrhålet.

Grundvattenflödesmätningar genomfördes i två enskilda sprickor och i två sprickzoner på nivåer från ca 232 till ca 422 m borrhålslängd (204 till 365 m vertikalt djup). Den hydrauliska transmissiviteten varierade inom intervallet $T = 8{,}9 \cdot 10^{-9}$–$5{,}5 \cdot 10^{-5}$ m$^2$/s. Resultaten från utspädningsmätningarna i borrhålet KFM04A visar att grundvattenflödet varierar avsevärt under naturliga, dvs ostörda, hydrauliska förhållanden. Den generella trenden är dock att flödet och Darcy hastigheten minskar med djupet. Beräknade grundvattenflöden låg inom intervallet 0,004–16,6 ml/min och Darcy hastigheterna varierade mellan $3{,}5 \cdot 10^{-10}$ och $3{,}6 \cdot 10^{-7}$ m/s ($3{,}0 \cdot 10^{-5}$–$3{,}1 \cdot 10^{-2}$ m/d). Resultaten överensstämmer med tidigare genomförda mätningar i Forsmark. Störst flöde och högsta Darcy hastighet uppmättes i sektionen med flera flödande sprickor i den övre delen av deformationszon ZFMNE00A2. Hydrauliska gradienter, beräknade enligt Darcy konceptet, ligger inom det förväntade området (0,001–0,05) i två av fyra testade sprickor/zoner. Grundvattenflödet är proportionellt mot den hydrauliska transmissiviteten, dock är det statistiska underlaget litet.

Ett försök gjordes också att utföra mätningar i två lågtransmissiva sektioner ($T < 10^{-9}$ m$^2$/s) på ca 517 m och ca 522 m borrhålslängd (442 och 446 m vertikalt djup). Dessvärre fick mätförsöken avbrytas på grund av tekniska problem i kombination med hög partikelhalt och den kemiska sammansättning i borrhålsvattnet vilka tillsammans orsakade igensättning av den optiska mätcellen.

SWIW testet genomfördes i övre delen av deformationszon ZFMNE1188 på ca 417 m borrhålslängd (361 m vertikalt djup) med $T = 8{,}9 \cdot 10^{-9}$ m$^2$/s.

De experimentella genombrottskurvorna uppvisar i detta fall flera avvikande egenskaper jämfört med tidigare SWIW-försök inom platsundersökningsprogrammen vilket väsentligt försvårade en kvantitativ modellutvärdering. Beräknad återhämtning av spårämnen är tämligen låg, 42,6 %, 53,9 % och 32,8 % för respektive Uranin, rubidium och cesium. Dessutom ger genombrottskurvan för cesium ett dubiöst intryck, där delar av kurvan indikerar mycket svag retention medan andra delar indikerar betydligt starkare retention. På grund av detta görs ingen skattning av retardationsfaktorn för cesium i denna rapport. Skattningar av retardationsfaktor för rubidium gav ett intervall från 2,9 till 5,5. Dessa värden bör dock ses som mycket osäkra.

# Contents

# 1 Introduction

SKB is currently conducting a site investigation for a deep repository in Forsmark, according to general and site specific programmes /SKB 2001ab/. Two, among several methods for site characterisation are in situ groundwater flow measurements and single well injection withdrawal tests (SWIW tests).

This document reports the results gained by a SWIW test and groundwater flow measurements with the borehole dilution probe in borehole KFM04A. The work was conducted by Geosigma AB and carried out between January 2006 and May 2006 in borehole KFM04A according to activity plan AP PF 400-06-002. In Table 1-1 controlling documents for performing this activity are listed. Both activity plans and method descriptions/instructions are SKB's internal controlling documents. Data and results were delivered to the SKB site characterization database SICADA.

Borehole KFM04A is located in the north western part of the investigation area, Figure 1-1. KFM04A is a telescopic borehole where the part below 100 m borehole length is core drilled. KFM04A is inclined –60.08° from the horizontal plane at collaring. The borehole is in total 1,001 m long and cased down to 108 m. From 108 m down to 1,001 m the diameter is 77 mm.

Detailed information about borehole KFM04A is listed in Appendix A (excerpt from the SKB database SICADA).

**Table 1-1. Controlling documents for performance of the activity.**

| **Activity plan** | **Number** | **Version** |
|---|---|---|
| Grundvattenflödesmätningar och SWIW-test KFM04A | AP PF 400-06-002 | 1.0 |
| **Method documents** | **Number** | **Version** |
| Metodbeskrivning för grundvattenflödesmätning | SKB MD 350.001 | 1.0 |
| Kalibrering av tryckgivare, temperaturgivare och flödesmätare | SKB MD 353.014 | 2.0 |
| Kalibrering av fluorescensmätning | SKB MD 353.015 | 2.0 |
| Kalibrering Elektrisk konduktivitet | SKB MD 353.017 | 2.0 |
| Utspädningsmätning | SKB MD 353.025 | 2.0 |
| Löpande och avhjälpande underhåll av Utspädningssond | SKB MD 353.065 | 1.0 |
| Systemöversikt – SWIW-test utrustning | SKB MD 353.069 | 1.0 |
| Löpande och avhjälpande underhåll av SWIW-test utrustning | SKB MD 353.070 | 1.0 |
| Kalibrering av flödesmätare i SWIW-test utrustning | SKB MD 353.090 | 1.0 |
| Instruktion för rengöring av borrhålsutrustning och viss markbaserad utrustning | SKB MD 600.004 | 1.0 |
| Instruktion för längdkalibrering vid undersökningar i kärnborrhål | SKB MD 620.010 | 1.0 |

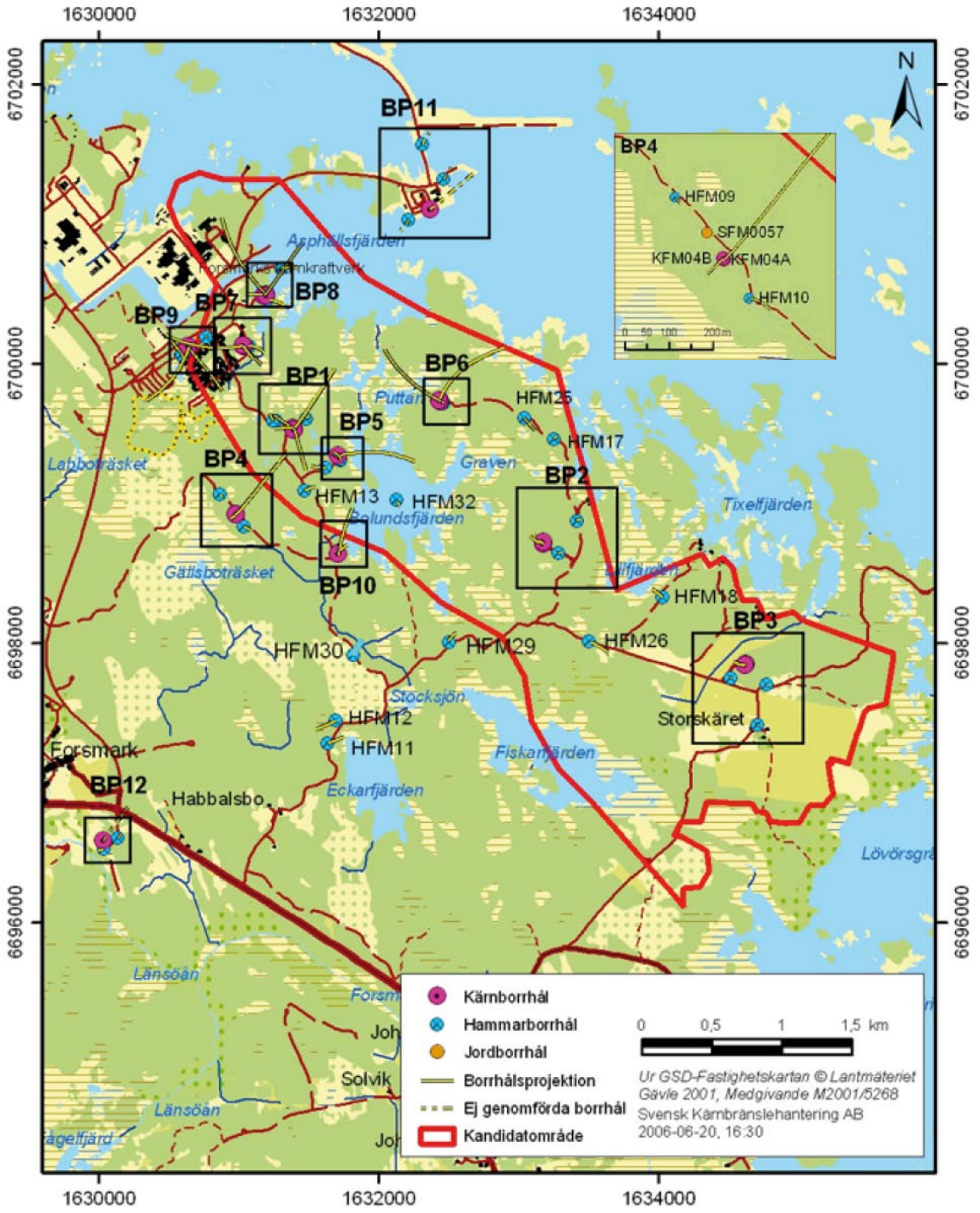


***Figure 1-1.*** *Overview of the Forsmark site investigation area, showing core boreholes (purple) and percussion boreholes (blue). A close-up of Drill Site 4 with KFM04A is shown in the upper right corner.*

# 2 Objectives and scope

One objective of the activity was to determine groundwater flow under natural gradient as well as hydraulic gradients in the Forsmark area.

The objective of the SWIW test was to determine transport properties of groundwater flow paths in fractures/fracture zones in a depth range of 300–700 m and a hydraulic transmissivity of $1 \cdot 10^{-8}$–$1 \cdot 10^{-6}$ $m^2/s$ in the test section. Since there is a great interest for data on transport properties in single fractures and fracture zones with low hydraulic transmissivity, such a section was chosen with $T = 8.9 \cdot 10^{-9}$ $m^2/s$ which is slightly below the measurement range of the equipment.

The groundwater flow measurements were performed in fractures and fracture zones at a borehole length range of 232–422 m (204–365 m vertical depth) using the SKB borehole dilution probe. The hydraulic transmissivity in the test sections ranged between $8.9 \cdot 10^{-9}$–$5.5 \cdot 10^{-5}$ $m^2/s$. Groundwater flow measurements were carried out in totally four test sections. In one of these sections a SWIW test was also conducted using both sorbing and non-sorbing tracers, simultaneously.

# 3 Equipment

## 3.1 Borehole dilution probe

The borehole dilution probe is a mobile system for groundwater flow measurements, Figure 3-1. Measurements can be made in boreholes with 56 mm or 76–77 mm diameter and the test section length can be arranged for 1, 2, 3, 4 or 5 m with an optimised special packer/dummy system and section lengths between 1 and 10 m with standard packers. The maximum measurement depth is at 1,030 m borehole length. The vital part of the equipment is the probe which measures the tracer concentration in the test section down hole and in situ. The probe is equipped with two different measurement devices. One is the Optic device, which is a combined fluorometer and light-transmission meter. Several fluorescent and light absorbing tracers can be used with this device. The other device is the Electrical Conductivity device, which measures the electrical conductivity of the water and is used for detection/analysis of saline tracers. The probe and the packers that straddle the test section are lowered down the borehole with an umbilical hose. The hose contains a tube for hydraulic inflation/deflation of the packers and electrical wires for power supply and communication/data transfer. Besides tracer dilution detection, the absolute pressure and temperature are measured. The absolute pressure is measured during the process of dilution because a change in pressure indicates that the hydraulic gradient, and thus the groundwater flow, may have changed. The pressure gauge and the temperature gauge are both positioned in the dilution probe, about seven metres from top of test section. This bias is not corrected for as only changes and trends relative to the start value are of great importance for the dilution measurement. Since the dilution method requires homogenous distribution of the tracer in the test section, a circulation pump is also installed and circulation flow rate measured.

A caliper log, attached to the dilution probe, is used to position the probe and test section at the pre-selected borehole length. The caliper detects reference marks previously made by a drill bit at exact length along the borehole, approximately every 50 m. This method makes it possible to position the test section with an accuracy of c. ± 0.10 m.

### 3.1.1 Measurement range and accuracy

The lower limit of groundwater flow measurement is set by the dilution caused by molecular diffusion of the tracer into the fractured/porous aquifer, relative to the dilution of the tracer due to advective groundwater flow through the test section. In a normally fractured granite, the lower limit of a groundwater flow measurement is approximately at a hydraulic conductivity, K, between $6 \cdot 10^{-9}$ and $4 \cdot 10^{-8}$ m/s, if the hydraulic gradient, I, is 0.01. This corresponds to a groundwater flux (Darcy velocity), v, in the range of $6 \cdot 10^{-11}$ to $4 \cdot 10^{-10}$ m/s, which in turn may be transformed into groundwater flow rates, $Q_w$, corresponding to 0.03–0.2 ml/hour through a one m test section in a 76 mm diameter borehole. In a fracture zone with high porosity, and thus a higher rate of molecular diffusion from the test section into the fractures, the lower limit is about $K = 4 \cdot 10^{-7}$ m/s if I = 0.01. The corresponding flux value is in this case $v = 4 \cdot 10^{-9}$ m/s and flow rate $Q_w = 2.2$ ml/hour. The lower limit of flow measurements is, however, in most cases constrained by the time available for the dilution test. The required time frame for an accurate flow determination from a dilution test is within 7–60 hours at hydraulic conductivity values greater than about $1 \cdot 10^{-7}$ m/s. At conductivity values below $1 \cdot 10^{-8}$ m/s, measurement times should be at least 70 hours for natural (undisturbed) hydraulic gradient conditions.

The upper limit of groundwater flow measurements is determined by the capability of maintaining a homogeneous mix of tracer in the borehole test section. This limit is determined by several factors, such as length of the test section, volume, distribution of the water conducting fractures and how the circulation pump inlet and outlet are designed. The practical upper measurement limit is about 2,000 ml/hour for the equipment developed by SKB.

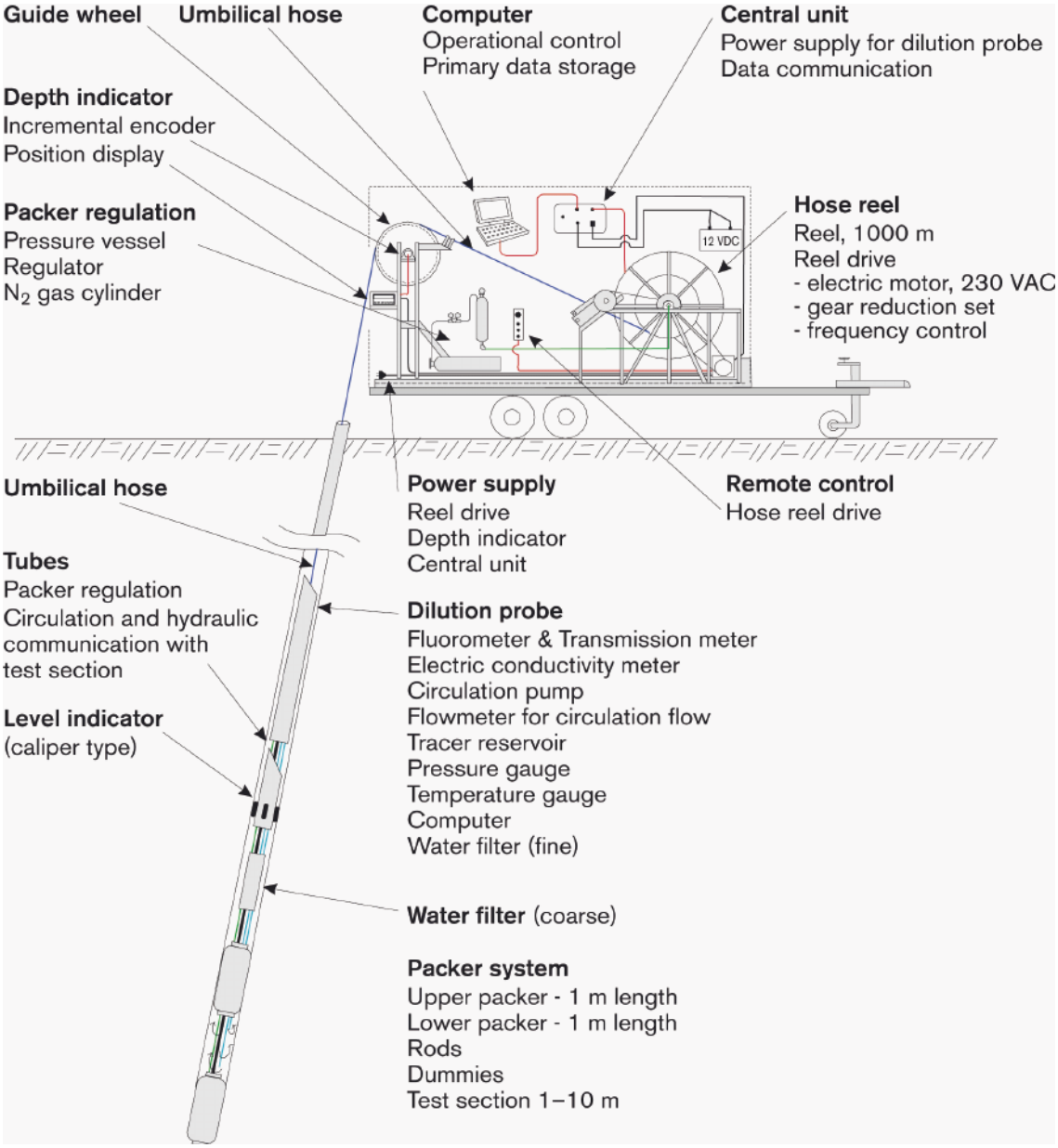


***Figure 3-1.*** *The SKB borehole dilution probe.*

The accuracy of determined flow rates through the borehole test section is affected by various measurement errors related to, for example, the accuracy of the calculated test section volume and determination of tracer concentration. The overall accuracy when determining flow rates through the borehole test section is better than ± 30%, based on laboratory measurements in artificial borehole test sections.

The groundwater flow rates in the rock formation are determined from the calculated groundwater flow rates through the borehole test section and by using some assumption about the flow field around the borehole test section. This flow field depends on the hydraulic properties close to the borehole and is given by the correction factor α, as discussed below in Section 4.4.1. The value of α will, at least, vary within $\alpha = 2 \pm 1.5$ in fractured rock /Gustafsson 2002/. Hence, the groundwater flow in the rock formation is calculated with an accuracy of about ± 75%, depending on the flow-field distortion.

## 3.2 SWIW test equipment

The SWIW (Single Well Injection Withdrawal) test equipment constitutes a complement to the borehole dilution probe making it possible to carry out a SWIW test in the same test section as the dilution measurement, Figure 3-2. Measurements can be made in boreholes with 56 mm or 76–77 mm diameter and the test section length can be arranged for 1, 2, 3, 4 or 5 m with an optimised special packer/dummy system for 76–77 mm boreholes. The equipment is primarily designed for measurements in the depth interval 300–700 m borehole length. However, measurements can be carried out at shallower depths as well at depths larger than 700 m. The possibility to carry out a SWIW test much depends on the hydraulic transmissivity in the investigated test section and frictional loss in the tubing at tracer withdrawal pumping. Besides the dilution probe, the main parts of the SWIW test equipment are:

- Polyamide tubing constituting the hydraulic connection between SWIW test equipment at ground surface and the dilution probe in the borehole.
- Air tight vessel for storage of groundwater under anoxic conditions, i.e. $N_2$-athmosphere.
- Control system for injection of tracer solution and groundwater (chaser fluid).
- Injection pumps for tracer solution and groundwater.

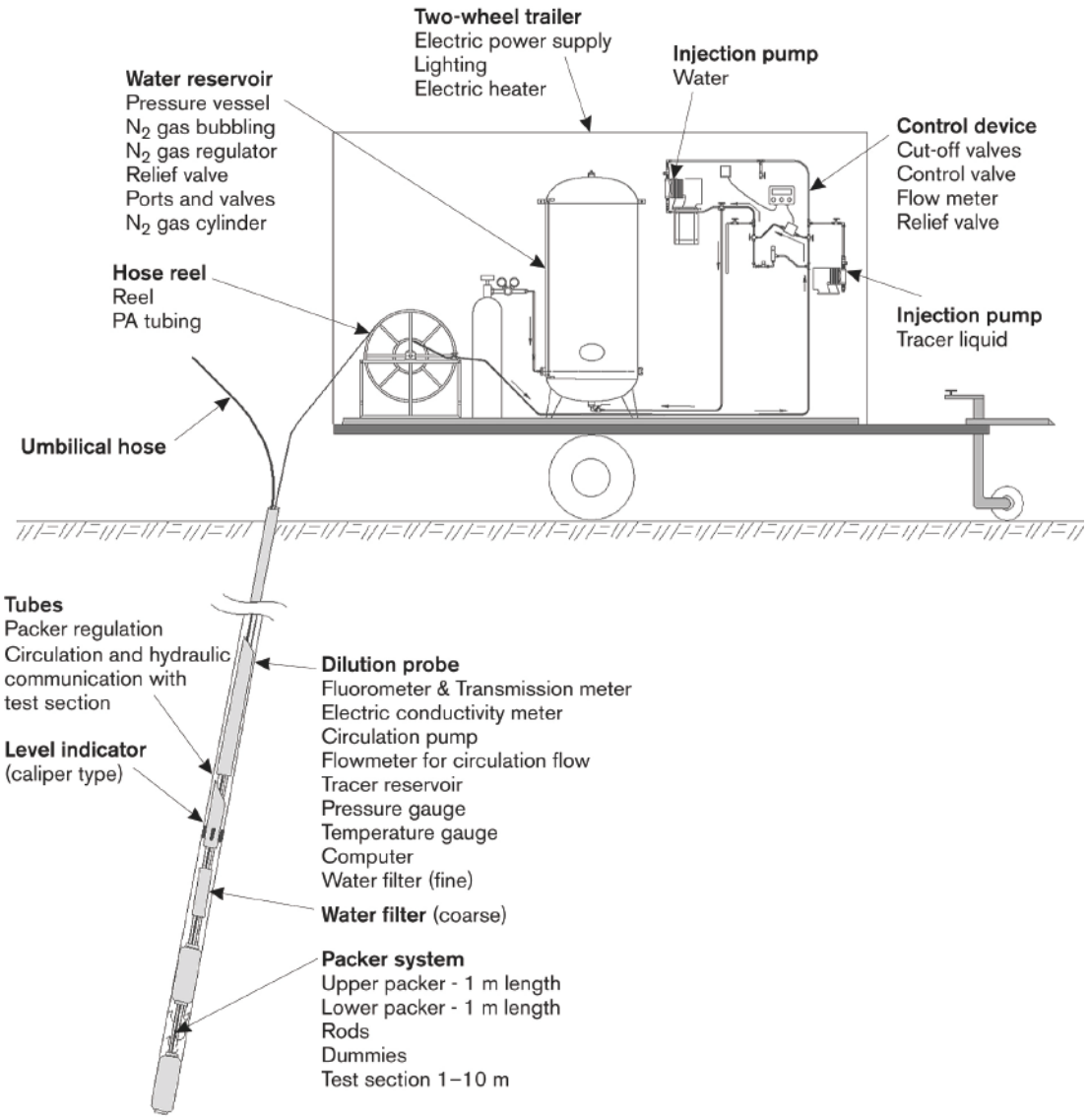


***Figure 3-2.*** *SWIW test equipment, connected to the borehole dilution probe.*

### 3.2.1 Measurement range and accuracy

The result of a SWIW test depends on the accuracy in the determination of the tracer concentration in injection solutions and withdrawn water. The result also depends on the accuracy in the volume of injection solution and volumes of injected and withdrawn water. For non-sorbing dye tracers (e.g. Uranine) the tracer concentration in collected water samples can be analysed with a resolution of 10 µg/l in the range 0.0–4.0 mg/l. The accuracy is within ± 5%. The volume injected tracer solution can be determined within ± 0.1% and the volume of injected and withdrawn water determined within 5%.

The evaluation of a SWIW test and determination of transport parameters is done with model simulations, fitting the model to the measured data (concentration as a function of time). The accuracy in determined transport parameters depends on selection of model concept and how well the model fit the measured data.

# 4 Execution

The measurements were performed according to AP PF 400-06-002 (SKB internal controlling document) in compliance with the methodology descriptions for the borehole dilution probe equipment – SKB MD 350.001, Metodbeskrivning för grundvattenflödesmätning –, and the measurement system description for SWIW test – SKB MD 353.069, MSB; Systemöversikt – SWIW-test utrustning – (SKB Internal controlling documents), Table 1-1.

## 4.1 Preparations

The preparations included calibration of the fluorometer and the electric conductivity meter before arriving at the site. Briefly, this was performed by adding certain amounts of the tracer to a known test volume while registering the measured A/D-levels. From this, calibration constants were calculated and saved for future use by using the measurement application. The other sensors had been calibrated previously and were hence only control calibrated.

Extensive functionality checks were accomplished prior to transport to the site and limited function checks were performed at the site. The equipment was cleaned to comply with SKB cleaning level 1 before lowering it into the borehole. All preparations were performed according to SKB Internal controlling documents, cf. Table 1-1.

## 4.2 Procedure

### 4.2.1 Groundwater flow measurement

In total four groundwater flow measurements were carried out, Table 4-1.

**Table 4-1. Performed dilution (flow) measurements.**

| Borehole | Test section (m)+ | Number of flowing fractures* | T ($m^2/s$) | Tracer | Test period (yymmdd–yymmdd) |
|---|---|---|---|---|---|
| KFM04A | 232.0–237.0 (204.0–208.3) | 3 | 5.50E–05* | Uranine | 060221–060223 |
| KFM04A | 296.5–297.5 (259.5–260.3) | 1 | 1.61E–07* | Uranine | 060120–060124 |
| KFM04A | 359.3–360.3 (312.9–313.7) | 1 | 1.26E–06* | Uranine | 060117–060120 |
| KFM04A | 417.0–422.0 (361.0–365.1) | 1–2 | 8.91E–09** | Uranine | 060124–060213 |

* /Rouhiainen and Pöllänen 2004/.

** /Hjerne and Ludvigson 2005/.

+ Test section vertical depth is given within brackets.

Each measurement was performed according to the following procedure. The equipment was lowered to the correct borehole length where background values of tracer concentration and supporting parameters, pressure and temperature, were measured and logged. Then, after inflating the packers and the pressure had stabilized, tracer was injected in the test section.The tracer concentration and supporting parameters were measured and logged continuously until the tracer had been diluted to such a degree that the groundwater flow rate could be calculated.

### 4.2.2 SWIW tests

One SWIW test was performed, Table 4-2. A BIPS image of the test section is shown in Appendix C. To conduct a SWIW test requires that the SWIW equipment is connected to the borehole dilution probe, Figures 3-1 and 3-2.

The SWIW test was carried out according to the following procedure. The equipment was lowered to the correct borehole length where background values of Uranine and supporting parameters, pressure and temperature, were measured and logged. Then, after inflating the packers and the pressure had stabilized, the circulation pump in the dilution probe was used to pump groundwater from the test section to the air tight vessel at ground surface. Water samples were also taken for analysis of background concentration of Uranine, rubidium and cesium. When pressure had recovered after the pumping in the test section, the injection phases started with pre-injection of the native groundwater to reach steady state flow conditions. Thereafter groundwater spiked with the tracers Uranine, rubidium and cesium was injected. Finally, injection of native groundwater to push the tracers out into the fracture/fracture zone was performed. The withdrawal phase started by pumping water to the ground surface. An automatic sampler at ground surface was used to take water samples for analysis of Uranine, rubidium and cesium in the withdrawn water.

## 4.3 Data handling

During groundwater flow measurement with the dilution probe, data are automatically transferred from the measurement application to a SQL database. Data relevant for analysis and interpretation are then automatically transferred from SQL to Excel via an MSSQL (ODBC) data link, set up by the operator. After each measurement the Excel data file is copied to a CD.

The water samples from the SWIW test were analysed for Uranine tracer content at the Geosigma Laboratory in Uppsala. Cesium and rubidium contents were analysed at the Analytica laboratory in Luleå.

**Table 4-2. Performed SWIW tests.**

| Borehole | Test section (m)+ | Number of flowing fractures* | T ($m^2/s$) | Tracers | Test period (yymmdd–yymmdd) |
|---|---|---|---|---|---|
| KFM04A | 417.0–422.0 (361.0–365.1) | 1–2 | 8.91E–09** | Uranine/cesium/ rubidium | 060223–060314 |

* /Rouhiainen and Pöllänen 2004/.

** /Hjerne and Ludvigson 2005/.

+ Test section vertical depth is given within brackets.

## 4.4 Analyses and interpretation

### 4.4.1 The dilution method – general principles

The dilution method is an excellent tool for in situ determination of flow rates in fractures and fracture zones.

In the dilution method a tracer is introduced and homogeneously distributed into a bore-hole test section. The tracer is subsequently diluted by the ambient groundwater, flowing through the borehole test section. The dilution of the tracer is proportional to the water flow through the borehole section, Figure 4-1.

The dilution in a well-mixed borehole section, starting at time t = 0, is given by:

$$\ln(C/C_0) = -\frac{Q_w}{V} \cdot t \qquad \text{(Equation 4-1)}$$

where C is the concentration at time t (s), $C_0$ is the initial concentration, V is the water volume ($m^3$) in the test section and $Q_w$ is the volumetric flow rate ($m^3/s$). Since V is known, the flow rate may then be determined from the slope of the line in a plot of ln ($C/C_0$), or ln C, versus t.

An important interpretation issue is to relate the measured groundwater flow rate through the borehole test section to the rate of groundwater flow in the fracture/fracture zone straddled by the packers. The flow-field distortion must be taken into consideration, i.e. the degree to which the groundwater flow converges and diverges in the vicinity of the borehole test section. With a correction factor, α, which accounts for the distortion of the flow lines due to the presence of the borehole, it is possible to determine the cross-sectional area perpendicular to groundwater flow by:

$$A = 2 \cdot r \cdot L \cdot \alpha \qquad \text{(Equation 4-2)}$$

where A is the cross-sectional area ($m^2$) perpendicular to groundwater flow, r is borehole radius (m), L is the length (m) of the borehole test section and α is the correction factor. Figure 4-2 schematically shows the cross-sectional area, A, and how flow lines converge and diverge in the vicinity of the borehole test section.

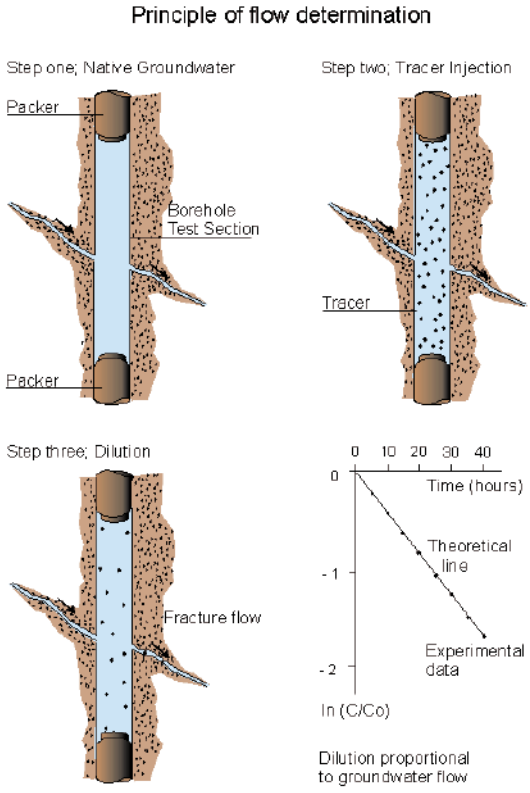


***Figure 4-1.*** *General principles of dilution and flow determination.*

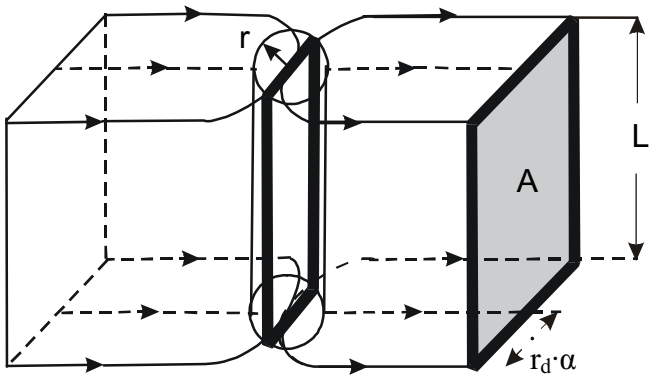


***Figure 4-2.*** *Diversion and conversion of flow lines in the vicinity of a borehole test section.*

Assuming laminar flow in a plane parallel fissure or a homogeneous porous medium, the correction factor α is calculated according to Equation (4-3), which often is called the formula of Ogilvi /Halevy et al. 1967/. Here it is assumed that the disturbed zone, created by the presence of the borehole, has an axis-symmetrical and circular form.

$$\alpha = \frac{4}{1 + (r/r_d) + (K_2/K_1)(1 - (r/r_d)^2)} \qquad \text{(Equation 4-3)}$$

where $r_d$ is the outer radius (m) of the disturbed zone, $K_1$ is the hydraulic conductivity (m/s) of the disturbed zone, and $K_2$ is the hydraulic conductivity of the aquifer. If the drilling has not caused any disturbances outside the borehole radius, then $K_1 = K_2$ and $r_d = r$ which will result in $\alpha = 2$. With $\alpha = 2$, the groundwater flow within twice the borehole radius will converge through the borehole test section, as illustrated in Figures 4-2 and 4-3.

If there is a disturbed zone around the borehole the correction factor α is given by the radial extent and hydraulic conductivity of the disturbed zone. If the drilling has caused a zone with a lower hydraulic conductivity in the vicinity of the borehole than in the fracture zone, e.g. positive skin due to drilling debris and clogging, the correction factor α will decrease. A zone of higher hydraulic conductivity around the borehole will increase α. Rock stress redistribution, when new boundary conditions are created by the drilling of the borehole, may also change the hydraulic conductivity around the borehole and thus affect α. In Figure 4-3, the correction factor, α, is given as a function of $K_2/K_1$ at different normalized radial extents of the disturbed zone ($r/r_d$). If the fracture/fracture zone and groundwater flow are not perpendicular to the borehole axis, this also has to be accounted for. At a 45 degree angle to the borehole axis the value of α will be about 41% larger than in the case of perpendicular flow. This is further discussed in /Gustafsson 2002, Rhén et al. 1991/.

In order to obtain the Darcy velocity in the undisturbed rock the calculated groundwater flow, $Q_w$ is divided by A, Equation 4-4.

$$v = Q_w / A \qquad \text{(Equation 4-4)}$$

The hydraulic gradient is then calculated as

$$I = v/K \qquad \text{(Equation 4-5)}$$

where K is the hydraulic conductivity.

### 4.4.2 The dilution method – evaluation and analysis

The first step of evaluation included studying a graph of the measured concentration versus time data. For further evaluation background concentration, i.e. any tracer concentration in the groundwater before tracer injection, was subtracted from the measured concentrations.

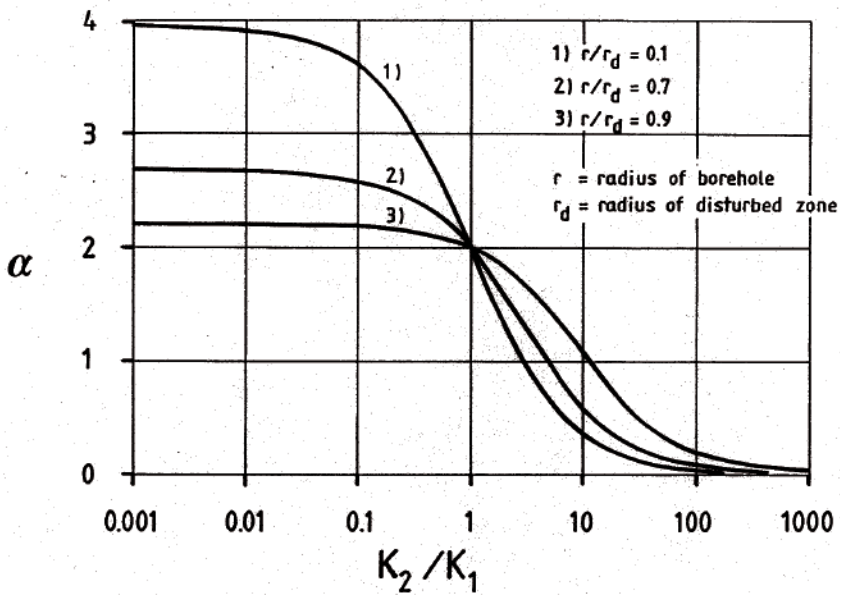


***Figure 4-3.*** *The correction factor, α, as a function of $K_2/K_1$ at different radial extent ($r/r_d$) of the disturbed zone (skin zone) around the borehole.*

Thereafter ln ($C/C_0$) was plotted versus time. In most cases that relationship was linear and the proportionality constant was then calculated by performing a linear regression. In the cases where the relationship between ln ($C/C_0$) and time was non-linear, a sub-interval was chosen in which the relationship was linear.

The value of ln ($C/C_0$)/t obtained from the linear regression was then used to calculate $Q_w$ according to Equation (4-1).

The hydraulic gradient, I, was calculated by combining Equations (4-2), (4-4) and (4-5), and choosing $\alpha = 2$. The hydraulic conductivity, K, in Equation (4-5) was obtained from previously performed Posiva Flow Log measurements (PFL) /Rouhiainen and Pöllänen 2004/ or Pipe String System measurements (PSS) /Hjerne and Ludvigson 2005/.

### 4.4.3 SWIW test – basic outline

A Single Well Injection Withdrawal (SWIW) test may consist of all or some of the following phases:

1. filling-up pressure vessel with groundwater from the selected fracture,
2. injection of water to establish steady state hydraulic conditions (pre-injection),
3. injection of one or more tracers,
4. injection of groundwater (chaser fluid) after tracer injection is stopped,
5. waiting phase,
6. withdrawal (recovery) phase.

The tracer breakthrough data used for evaluation are obtained from the withdrawal phase. The injection of chaser fluid, i.e. groundwater from the pressure vessel, has the effect of pushing the tracer out as a "ring" in the formation surrounding the tested section. This is generally a benefit, because when the tracer is pumped back, both ascending and descending parts are obtained in the recovery breakthrough curve. During the waiting phase there is no injection or withdrawal of fluid. The purpose of this phase is to increase the time available for time-dependent transport-processes so that these may be more easily evaluated from the resulting breakthrough curve. A schematic example of a resulting breakthrough curve during a SWIW test is shown in Figure 4-4.

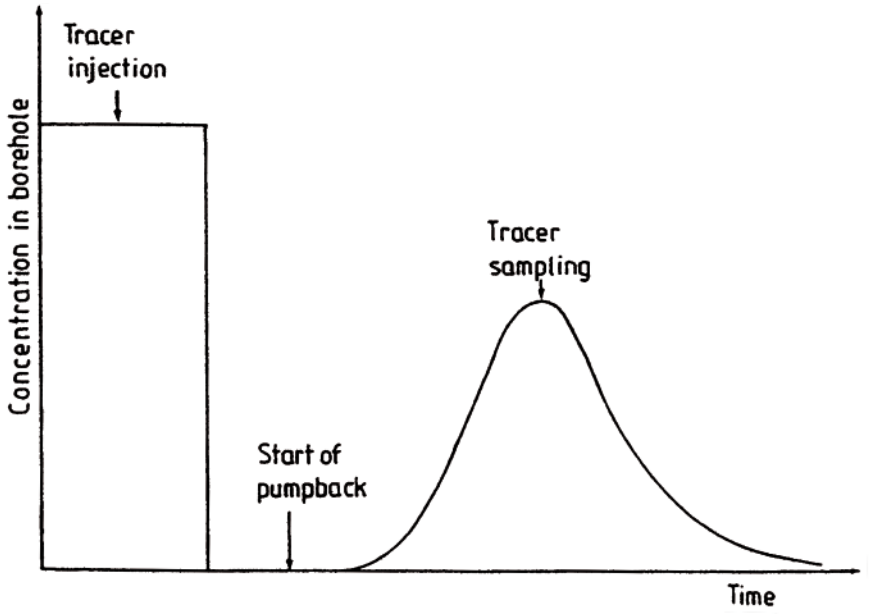


***Figure 4-4.*** *Schematic tracer concentration sequence during a SWIW test /Andersson, 1995/.*

The design of a successful SWIW test requires prior determination of injection and withdrawal flow rates, duration of tracer injection, duration of the various injections, waiting and pumping phases, selection of tracers, tracer injection concentrations, etc.

### 4.4.4 SWIW test – evaluation and analysis

The model evaluation of the experimental results was carried out assuming homogenous conditions. Model simulations were made using the model code SUTRA /Voss 1984/ and the experiments were simulated without a background hydraulic gradient. It was assumed that flow and transport occur within a planar fracture zone of some thickness. The volume available for flow was represented by assigning a porosity value to the assumed zone. Modelled transport processes include advection, dispersion and linear equilibrium sorption.

The sequence of the different injection phases was modelled as accurately as possible based on supporting data for flows and tracer injection concentration. Generally, experimental flows and times may vary from one phase to another, and the flow may also vary within phases. The specific experimental sequences for the borehole sections are listed below.

In the simulation model, tracer injection was simulated as a function accounting for mixing in the borehole section and sorption (for cesium and rubidium) on the borehole walls. The function assumes a completely mixed borehole section and linear equilibrium surface sorption:

$$C = (C_0 - C_{in})e^{-(\frac{Q}{V_{bh}+K_a A_{bh}})t} + C_{in} \qquad \text{(Equation 4-6)}$$

where C is concentration in water leaving the borehole section and entering the formation ($kg/m^3$), $V_{bh}$ is the borehole volume including circulation tubes ($m^3$), $A_{bh}$ is area of borehole walls ($m^2$), $Q_{in}$ is flow rate ($m^3/s$), $C_{in}$ is concentration in the water entering the borehole section ($kg/m^3$), $C_0$ is initial concentration in the borehole section ($kg/m^3$), $K_a$ is surface sorption coefficient (m) and t is elapsed time (s).

Based on in situ experiments /Andersson et al. 2002/ and laboratory measurements on samples of crystalline rock /Byegård and Tullborg 2005/ the sorption coefficient Ka was assigned a value of $10^{-2}$ m in all simulations. An example of the tracer injection input function is given in Figure 4-5, showing a 50 minutes long tracer injection phase followed by a chaser phase.

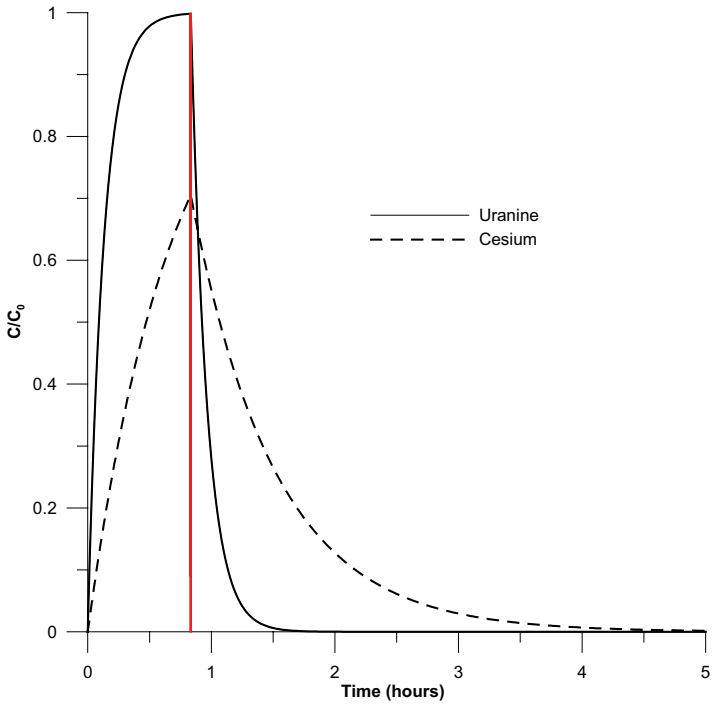


***Figure 4-5.*** *Example of simulated tracer injection functions for a tracer injection phase (ending at 50 minutes shown by the vertical red line) immediately followed by a chaser phase.*

Non-linear regression was used to fit the simulation model to experimental data. The estimation strategy was generally to estimate the dispersivity ($a_L$) and a retardation factor (R), while setting the porosity (i.e. the available volume for flow) to a fixed value. Simultaneous fitting of both tracer breakthrough curves (Uranine and cesium in the example), and calculation of fitting statistics, was carried out using the approach described in /Nordqvist and Gustafsson 2004/. Tracer breakthrough curves for Uranine and rubidium are related and calculated in the same way.

## 4.5 Nonconformities

The borehole water was found to have a high particle content and chemical composition that caused clogging of the optical measurement device. Hoisting of the borehole probe for cleaning and shifting of measurement technique/tracer, aiming to achieve reliable groundwater flow measurements, took some time and delayed the measurements. At 417–422 m borehole length three attempts were made to measure the groundwater flow. The first effort gave an apparent increase of groundwater flow after 75 hours of elapsed time due to the clogging of the optical device and only the first part of the dilution was used for final evaluation. Aiming at getting groundwater flow measurement of higher quality a second attempt with Uranine as tracer was made after establishing a new calibration of the optical device that agrees better with the conditions in the borehole. This second attempt gave an immediate clogging and could not be used for further evaluation. In the third attempt the tracer NaCl and the electric conductivity device were used in the section to avoid the problems with particles in the borehole water. This measurement gave unrealistic and scattered data and was not used for further evaluation. Eventually the first measurement was used for calculation of groundwater flow.

At 517–522 m borehole length one measurement attempt was made with NaCl as tracer. The dilution curve shows an unrealistic pattern with a top concentration much higher than theoretically possible. The equipment was hoisted, the optical device cleaned, a new calibration performed and an attempt to measure with Uranine as tracer was made. Once again clogging of

the optical device prevented a successful dilution measurement. The measurement efforts at this section and 522–527 m were therefore stopped.

The reference marks at 400 m could not be detected the second time a measurement was to be started in section 417.0–422.0 m. Reference marks from the first lowering was used instead.

Repeated problems with lowering the equipment past the transition cone between the upper, percussion drilled and the lower core drilled part of the borehole, and hoisting and lowering the equipment in the borehole occurred. At c. 440 m borehole length the equipment got stuck. A tractor had to be used to pull up the equipment. A screw between the 2 and 3 m dummies appeared to be missing and had probably got stuck between the borehole wall and the equipment.

The recovery pumping in the SWIW test was interrupted before the test was concluded due to a power failure. The last samples were taken from the SWIW hose.

# 5 Results

The primary data and original results are stored in the SKB database SICADA, where they are traceable by Activity Plan number. These data shall be used for further interpretation or modelling.

## 5.1 Dilution measurements

Figure 5-1 exemplifies a typical dilution curve in a fracture zone straddled by the test section at 232.0–237.0 m borehole length (204.0–208.3 m vertical depth) in borehole KFM04A. In the first phase the background value is recorded for about one hour. In phase two, Uranine tracer is injected, and after mixing a start concentration ($C_0$) of about 0.58 mg/l is achieved. In phase three the dilution is measured for about 18 hours. Thereafter the packers are deflated and the remaining tracer flows out of the test section. Figure 5-2 shows the measured pressure during the dilution measurement. Since the pressure gauge is positioned about seven metres from top of test section there is a bias from the pressure in the test section which is not corrected for, as only changes and trends relative to the start value are of great importance for the dilution measurement. Figure 5-3 is a plot of the ln ($C/C_0$) versus time data and linear regression best fit to data showing a good fit with correlation $R^2 = 0.9994$. The standard deviation, STDAV, shows the mean divergence of the values from the best fit line and is calculated from

$$\text{STDAV} = \sqrt{\frac{n\sum x^2 - \left(\sum x\right)^2}{n(n-1)}} \qquad \text{(Equation 5-1)}$$

Calculated groundwater flow rate, Darcy velocity and hydraulic gradient are presented in Table 5-1 together with the results from all other dilution measurements carried out in borehole KFM04A.

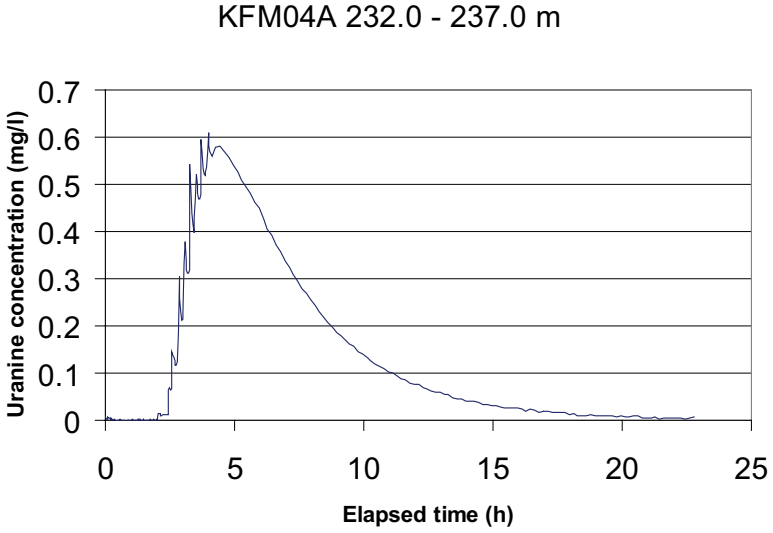


***Figure 5-1.*** *Dilution measurement in borehole KFM04A, section 232.0–237.0 m. Uranine concentration versus time.*

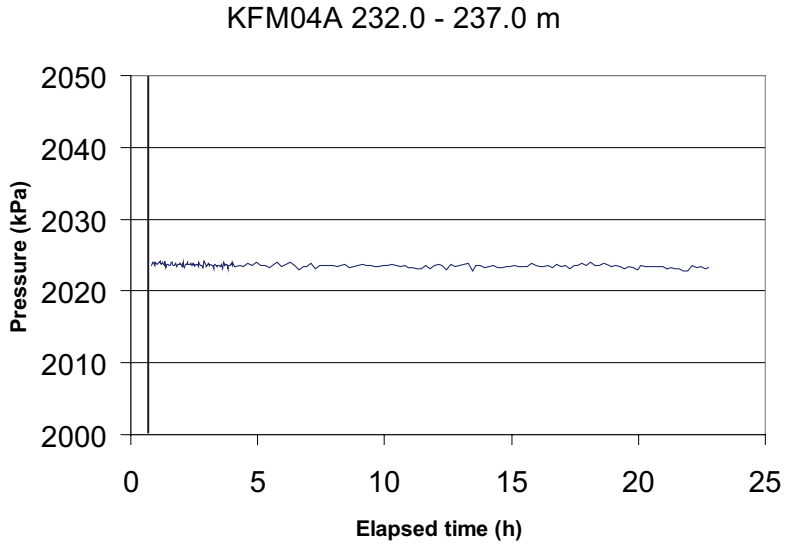


***Figure 5-2.*** *Measured pressure during dilution measurement in borehole KFM04A, section 232.0–237.0 m.*

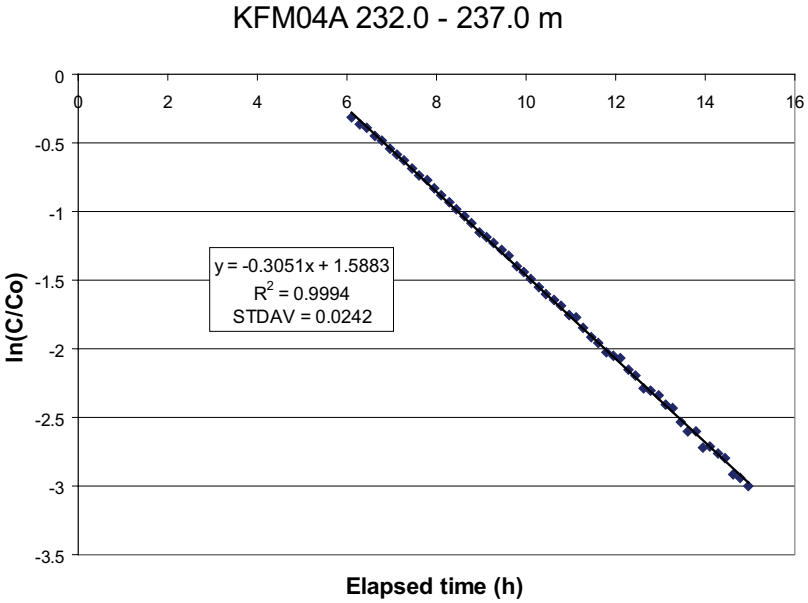


***Figure 5-3.*** *Linear regression best fit to data from dilution measurement in borehole KFM04A, section 232.0–237.0 m.*

The dilution measurements were carried out either with the dye tracer Uranine or the saline tracer NaCl. Uranine tracer was the first choice because it normally has a low background concentration and the tracer can be injected and measured in concentrations far above the background value, which gives a large dynamic range and accurate flow determinations. However, in some test sections precipitations and groundwater composition made it impossible to perform in situ measurements of Uranine with the fluorescence technique, which is an optical method. NaCl tracer, measured by means of electric conductivity, was then used instead. The drawback with NaCl measurements is the high background concentration at larger depth. Changes in the background concentration may have an influence on the measured tracer concentration in the test section, and thus also on the determined groundwater flow rate.

Details of all dilution measurements, with diagrams of dilution versus time and the supporting parameters pressure, temperature and circulation flow rate are presented in Appendix B1–B4.

### 5.1.1 KFM04A, section 232.0–237.0 m

This dilution measurement was carried out in a test section with three flowing fractures. The complete test procedure can be followed in Figure 5-1. Background concentration (0.003 mg/l) is measured for about one hour. Thereafter the Uranine tracer is injected in nine steps, and after mixing it finally reaches a start concentration of 0.58 mg/l above background. Dilution is measured for about 18 hours, the packers are then deflated. Hydraulic pressure is stable (Figure 5-2 and Appendix B1). The concentration reaches a level near background at the end of the dilution measurement. For this reason the latter part was excluded and the final evaluation was made on the 6 to 15 hours part of the dilution curve. The regression line fits well to the slope of the dilution with a correlation coefficient of $R^2 = 0.9994$ for the best fit line (Figure 5-3). The groundwater flow rate, calculated from the best fit line, is 16.6 ml/min. Calculated hydraulic gradient is 0.033 and Darcy velocity $3.6 \cdot 10^{-7}$ m/s.

### 5.1.2 KFM04A, section 296.5–297.5 m

This dilution measurement was carried out with the dye tracer Uranine in a test section with a single flowing fracture. The background measurement, tracer injection and dilution can be followed in Figure 5-4. Background concentration is 0.007 mg/l. The Uranine tracer is injected in three steps and after mixing it reaches a start concentration of 0.89 mg/l above background. Dilution is measured for about 90 hours, thereafter the packers are deflated and the remaining tracer flows out of the test section. Hydraulic pressure is stable but shows small diurnal pressure variations due to earth tidal effects (Appendix B2). Groundwater flow is determined from the 10–90 hours part of the dilution measurement. The correlation coefficient of the best fit line is $R^2 = 0.8332$ (Figure 5-5), and the groundwater flow rate, calculated from the best fit line, is 0.004 ml/min. Calculated hydraulic gradient is 0.003 and Darcy velocity $4.6 \cdot 10^{-10}$ m/s.

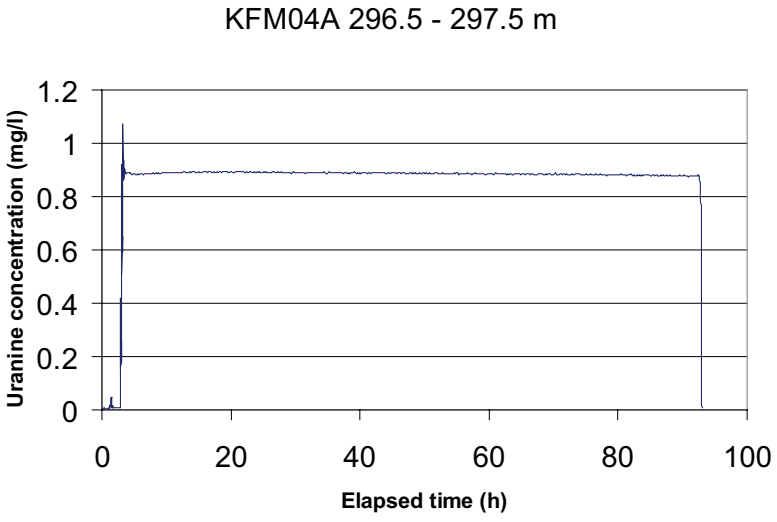


***Figure 5-4.*** *Dilution measurement in borehole KFM04A, section 296.5–297.5 m. Uranine concentration versus time.*

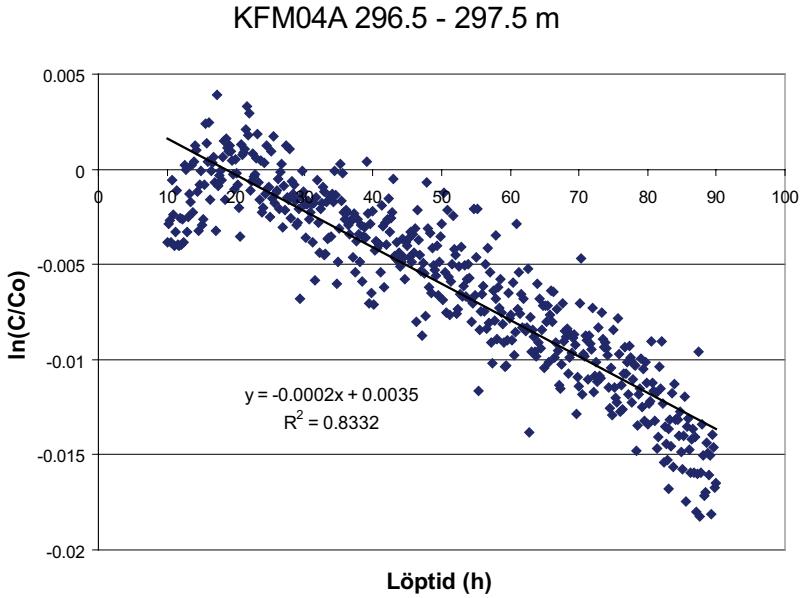


***Figure 5-5.*** *Linear regression best fit to data from dilution measurement in borehole KFM04A , section 296.5–297.5 m.*

### 5.1.3 KFM04A, section 359.3–360.3 m

This dilution measurement was carried out in a test section with a single flowing fracture. The background measurement, tracer injection and dilution can be followed in Figure 5-6. Background concentration (0.006 mg/l) is measured for about 50 minutes with the packers inflated. The Uranine tracer is injected in six steps and after mixing it reaches a start concentration of 0.47 mg/l above background. Dilution is measured for about 45 hours. Thereafter the packers are deflated and the remaining tracer flows out of the test section. Hydraulic pressure shows a decreasing trend at the beginning (Appendix B3). The final evaluation was made from 50 to 67 hours of elapsed time when the pressure is stabilised. The regression line fits well to the slope of the dilution with a correlation coefficient of $R^2 = 0.9984$ for the best fit line (Figure 5-7). The groundwater flow rate, calculated from the best fit line, is 0.96 ml/min.

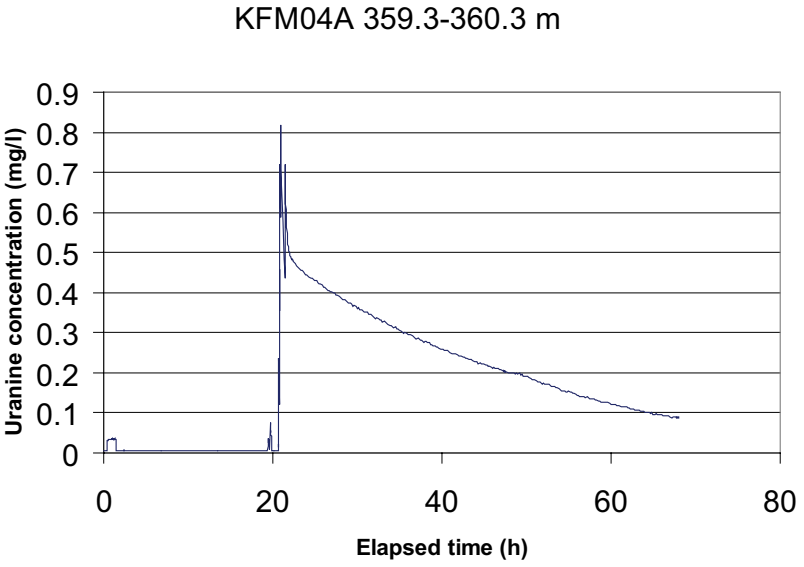


***Figure 5-6.*** *Dilution measurement in borehole KFM04A, section 359.3–360.3 m. Uranine concentration versus time.*

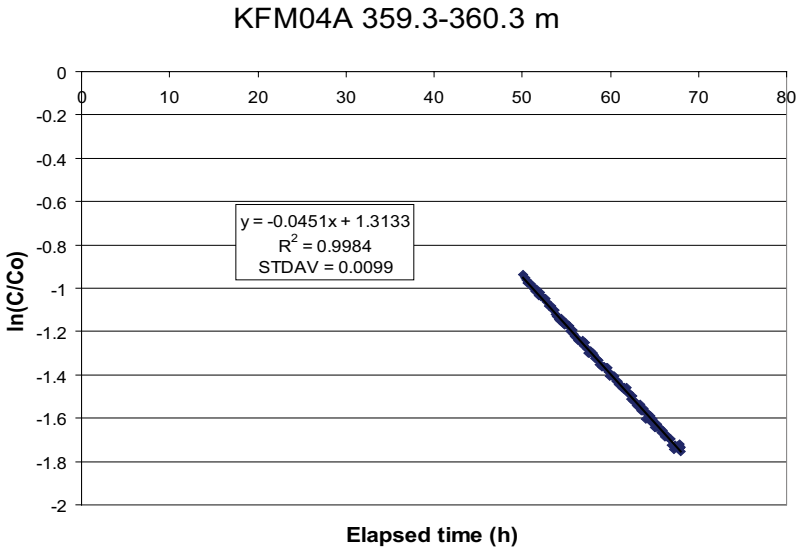


***Figure 5-7.*** *Linear regression best fit to data from dilution measurement in borehole KFM04A, section 359.3–360.3 m.*

Calculated hydraulic gradient is 0.082 and Darcy velocity $1.0 \cdot 10^{-7}$ m/s. The hydraulic gradient is large and may be caused by local effects, where the measured fracture constitutes a hydraulic conductor between other fractures with different hydraulic heads, or wrong estimates of the correction factor, α, and/or the hydraulic conductivity of the fracture.

### 5.1.4 KFM04A, section 417.0–422.0 m

This dilution measurement was carried out with the dye tracer Uranine in a test section with one-two flowing fractures. The background measurement, tracer injection and dilution can be followed in Figure 5-8. Background concentration (0.006 mg/l) is measured for about one hour. Thereafter the Uranine tracer is injected in three steps and after mixing it finally reaches a start concentration of 0.68 mg/l above background. Dilution is measured for about 145 hours. Thereafter the packers are deflated and the remaining tracer flows out of the test section.

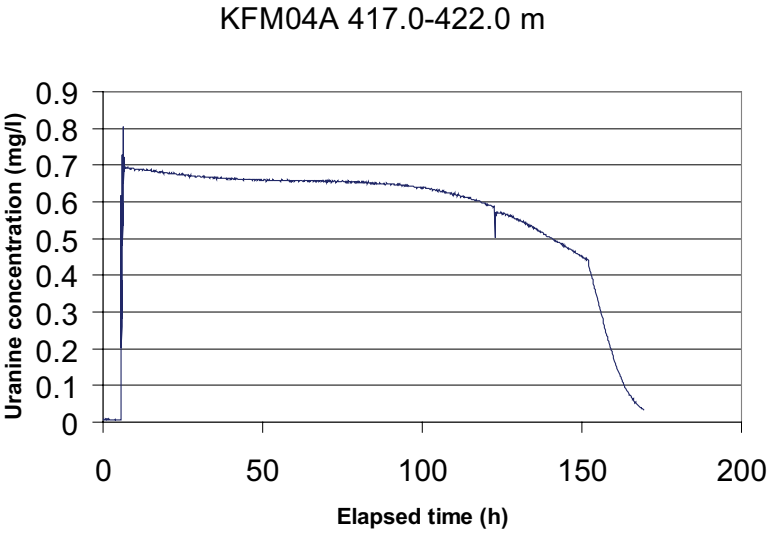


***Figure 5-8.*** *Dilution measurement in borehole KFM04A, section 417.0–422.0 m. Uranine concentration versus time.*

Hydraulic pressure shows a slow decreasing trend and small diurnal pressure variations due to earth tidal effects (Appendix B4). The borehole water was found to have high particle content and a chemical composition which caused a clogging of the optical device. Therefore, the latter part of the dilution curve was excluded and the final evaluation was made on the 37 to 75 hours part of the dilution curve where the pressure is stable and the clogging not influences the measurement. The regression line shows an acceptable fit to the ln ($C/C_0$) versus time data with a correlation coefficient of $R^2 = 0.7629$ for the best fit line (Figure 5-9). The groundwater flow rate, calculated from the best fit line, is 0.016 ml/min. Calculated hydraulic gradient is 0.20 and Darcy velocity $3.5 \cdot 10^{-10}$ m/s. The hydraulic gradient is large and may be caused by a hydraulic shortcut or wrong estimates of the correction factor, α, and/or the hydraulic conductivity as discussed in Section 5.1.3. The pressure decrease at the beginning of the measurement and the clogging of the optical device due to the particle content and chemical composition in the water may give some contribution to the estimated large hydraulic gradient. The hydraulic transmissivity of the section is at lower limit of measurement range for the dilution probe which may decrease the accuracy in the determined groundwater flow rate.

### 5.1.5 Summary of dilution results

Calculated groundwater flow rates, Darcy velocities and hydraulic gradients from all dilution measurements carried out in borehole KFM04A are presented in Table 5-1.

The results show that the groundwater flow varies considerably in fractures and fracture zones during natural, i.e. undisturbed, conditions, with flow rates from 0.004 to 16.6 ml/min and Darcy velocities from $3.5 \cdot 10^{-10}$ to $3.6 \cdot 10^{-7}$ m/s. The highest flow rate and Darcy velocity is measured in the upper part of the deformation zone ZFMNE00A2 at 232–237 m borehole length (204.0–208.3 m vertical depth). The lowest flow rate is measured in the low transmissive single fracture at c. 296 m borehole length (c. 260 m vertical depth) and the lowest Darcy velocity is measured in the deformation zone ZFMNE1188 at 417–422 m borehole length (361.0–365.1 m vertical depth), see Figures 5-10 and 5-11. Correlation between flow rate and transmissivity is indicated in Figure 5-13, with the highest flow rates at high transmissivity. Hydraulic gradients, calculated according to the Darcy concept, are large in the sections at c. 417 m and c. 359 m (361 and 313 m vertical depth), Figure 5-12. In the other measured fractures/fracture zones the hydraulic gradient is within the expected range. It is not clear if the large gradients are caused

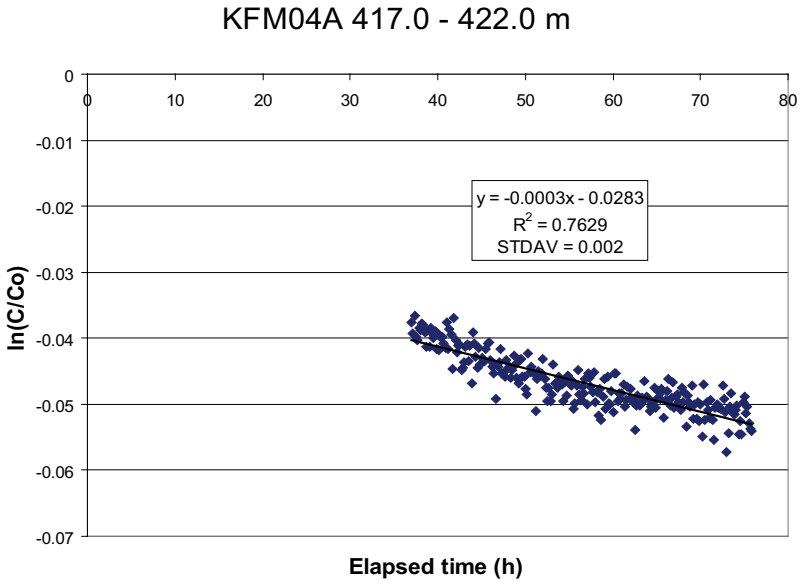


***Figure 5-9.*** *Linear regression best fit to data from dilution measurement in borehole KFM04A, section 417.0–422.0 m.*

**Table 5-1. Groundwater flow rates, Darcy velocities and hydraulic gradients for all measured sections in borehole KFM04A.**

| Borehole | Test section (m)+ | Number of flowing fractures* | T ($m^2/s$) | Q (ml/min) | Q ($m^3/s$) | Darcy velocity (m/s) | Hydraulic gradient |
|---|---|---|---|---|---|---|---|
| KFM04A | 232.0–237.0 (204.0–208.3) | 3 | 5.50E–05* | 16.6 | 2.8E–07 | 3.6E–07 | 0.033 |
| KFM04A | 296.5–297.5 (259.5–260.3) | 1 | 1.61E–07* | 0.004 | 7.1–E11 | 4.6E–10 | 0.003 |
| KFM04A | 359.3–360.3 (312.9–313.7) | 1 | 1.26E–06* | 0.96 | 1.6E–08 | 1.0E–07 | 0.082 |
| KFM04A | 417.0–422.0 (361.0–365.1) | 1–2 | 8.91E–09** | 0.016 | 2.7E–10 | 3.5E–10 | 0.198 |

* /Rouhiainen and Pöllänen 2004/.

** /Hjerne and Ludvigson 2005/.

+ Test section vertical depth is given within brackets.

by local effects where the measured fractures constitute hydraulic conductors between other fractures with different hydraulic heads or due to wrong estimates of the correction factor, α, and/or the hydraulic conductivity of the fracture. The pressure decrease at the beginning of the measurement and the clogging of the optical device may give some contribution to the large hydraulic gradient in the section at c. 417 m (361 m vertical depth). The hydraulic transmissivity of the section is at the lower limit of measurement range for the dilution probe which may decrease accuracy in determined groundwater flow rate.

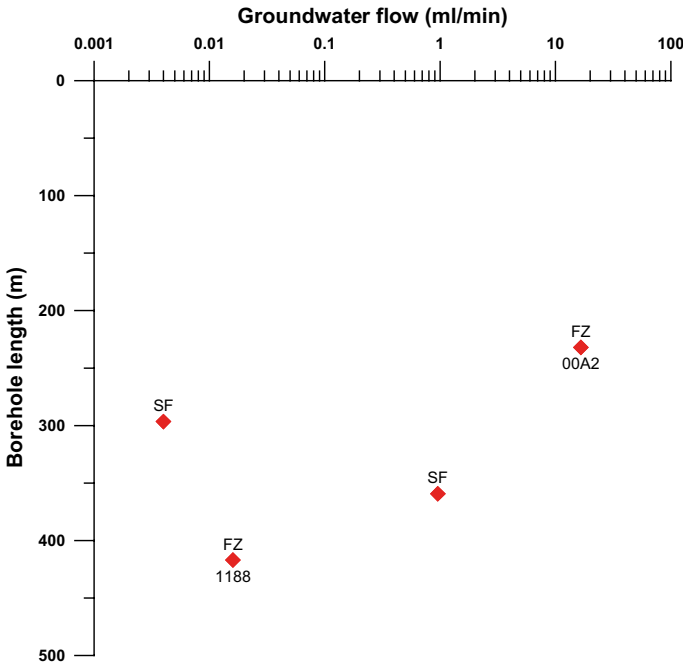


***Figure 5-10.*** *Groundwater flow rate versus borehole length during natural hydraulic gradient conditions. Results from dilution measurements in single fractures (SF) and fracture zones (FZ) in borehole KFM04A. Labels 00A2 and 1188 refer to fracture zone notation in the Forsmark site description model SDM F2.1 /SKB 2006/.*

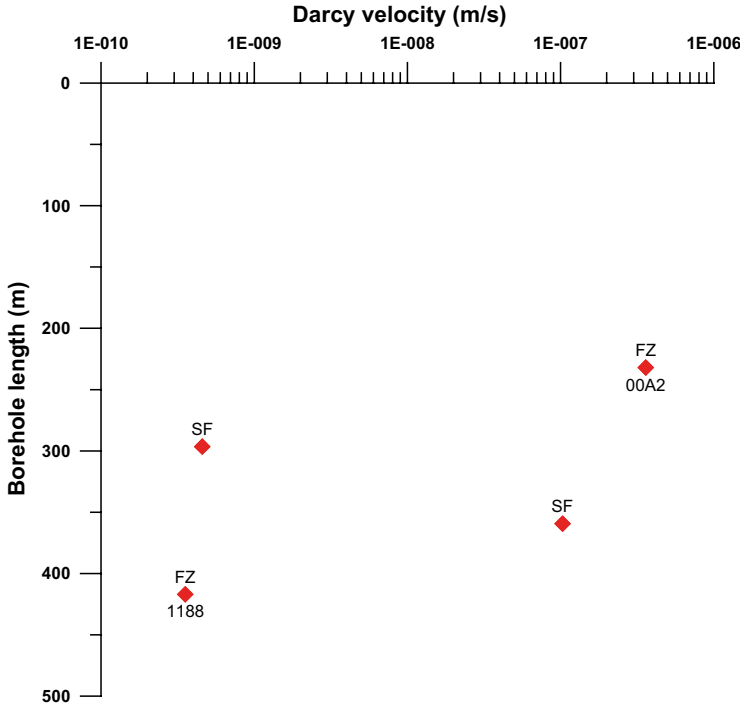


***Figure 5-11.*** *Darcy velocity versus borehole length during natural hydraulic gradient conditions. Results from dilution measurements in single fractures (SF) and fracture zones (FZ) in borehole KFM04A. Labels 00A2 and 1188 refer to fracture zone notation in the Forsmark site description model SDM F2.1 /SKB 2006/.*

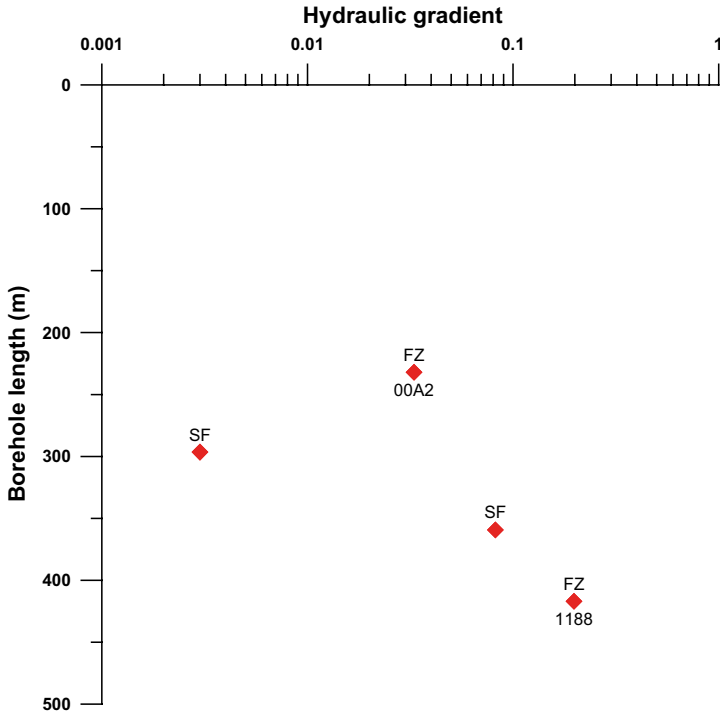


***Figure 5-12.*** *Hydraulic gradient versus borehole length during natural hydraulic gradient conditions. Results from dilution measurements in single fractures (SF) and fracture zones (FZ) in borehole KFM04A. Labels 00A2 and 1188 refer to fracture zone notation in the Forsmark site description model SDM F2.1 /SKB 2006/.*

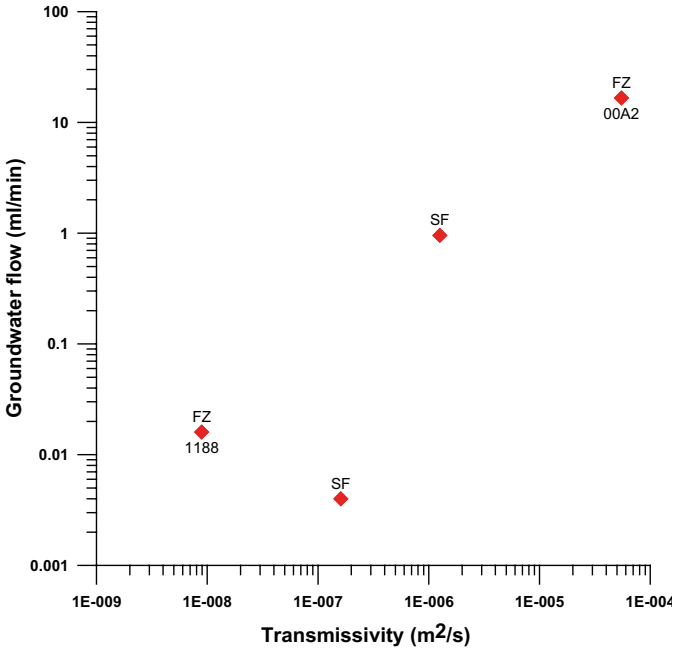


***Figure 5-13.*** *Groundwater flow rate versus transmissivity during undisturbed, i.e. natural hydraulic gradient conditions. Results from dilution measurements in single fractures (SF) and fracture zones (FZ) in borehole KFM04A. Labels 00A2 and 1188 refer to fracture zone notation in the Forsmark site description model SDM F2.1 /SKB 2006/.*

## 5.2 SWIW tests

### 5.2.1 Treatment of experimental data

The experimental data presented in this section have been corrected for background concentrations. Sampling times have been adjusted to account for residence times in injection and sampling tubing. Thus, time zero in all plots refers to when the fluid containing the tracer mixture begins to enter the tested borehole section.

### 5.2.2 Tracer recovery breakthrough in KFM04A, 417.0–422.0 m

Durations and flows for the various experimental phases are summarised in Table 5-2.

The experimental breakthrough curves from the recovery phase for Uranine, rubidium, and cesium, respectively, are shown in Figures 5-14a to 5-14c. The time coordinates are corrected for residence time in the tubing, as described above, and concentrations are normalised through division by the total injected tracer mass.

**Table 5-2. Durations (h) and fluid flows (L/h) during various experimental phases for section 417.0–422.0 m in borehole KFM04A. All times have been corrected for tubing residence time such that time zero refers to the time when the tracer mixture begins to enter the borehole section.**

| Phase | Start (h) | Stop (h) | Volume (L) | Average flow (L/h) | Cumulative injected volume (L) |
|---|---|---|---|---|---|
| Pre-injection | –5.52 | 0.00 | 13.43 | 2.43 | 13.43 |
| Tracer injection | 0.00 | 3.98 | 9.35 | 2.35 | 22.78 |
| Chaser injection | 3.98 | 70.01 | 148.6 | 2.25 | 171.38 |
| Recovery | 70.06 | 421.2 | 793.6 | 2.26 | |

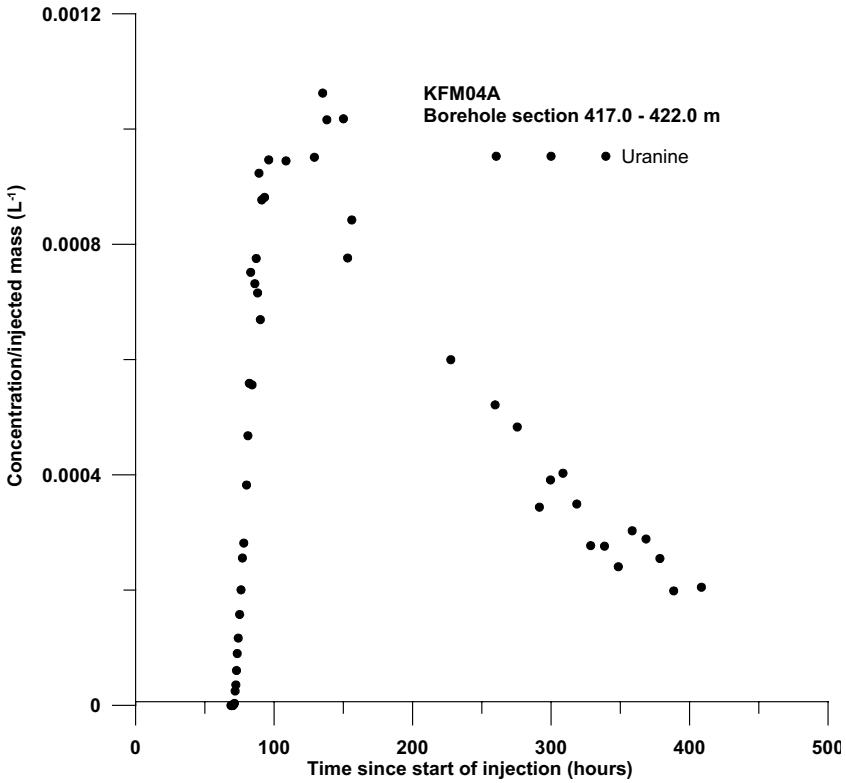


***Figure 5-14a.*** *Normalised withdrawal (recovery) phase breakthrough curve for Uranine in section 417.0–422.0 m in borehole KFM04A.*

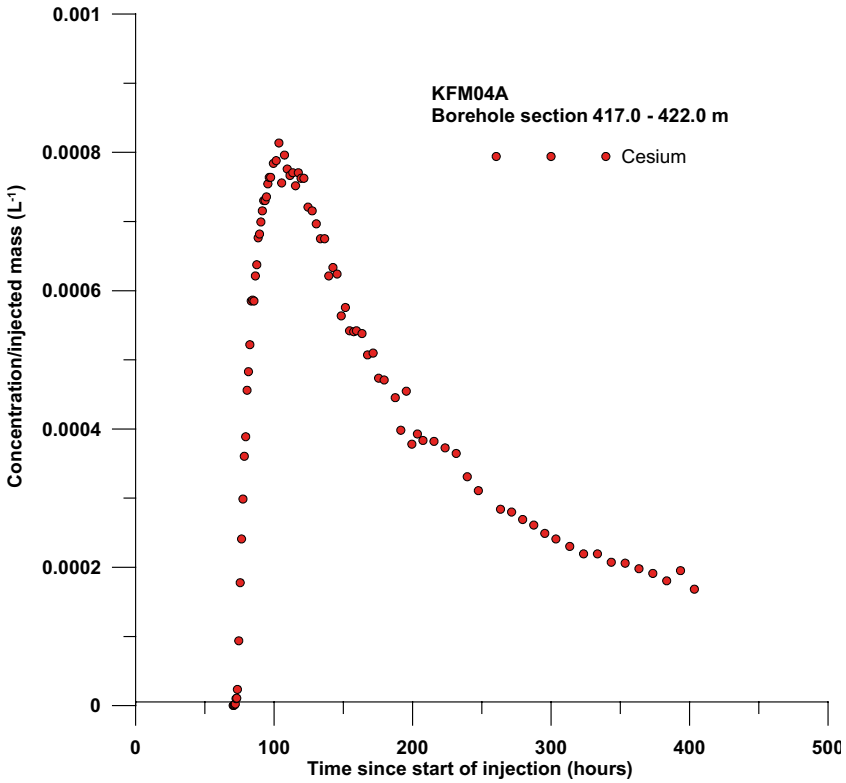


***Figure 5-14b.*** *Normalised withdrawal (recovery) phase breakthrough curve for cesium in section 417.0–422.0 m in borehole KFM04A.*

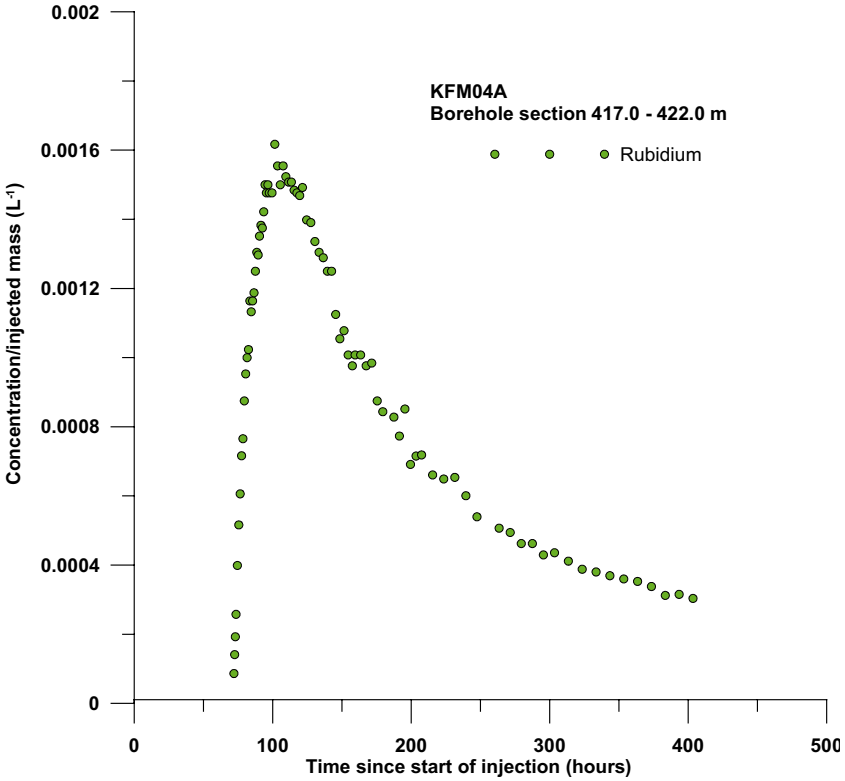


***Figure 5-14c.*** *Normalised withdrawal (recovery) phase breakthrough curve for rubidium in section 417.0–422.0 m in borehole KFM04A.*

Normalised breakthrough curves (concentration divided by total injected tracer mass) for all three tracers are plotted in Figure 5-15. The figure shows that the tracers behave in different ways, presumably caused by different sorption properties. However, the breakthrough curves differ significantly from what would be expected from a SWIW test using tracers of different sorption properties (assuming linear equilibrium sorption). This is also different compared with previously performed SWIW tests within the site investigation programmes /Gustafsson and Nordqvist 2005, Gustafsson et al. 2005, Gustafsson et al. 2006ab/, where the appearance of breakthrough curves for sorbing tracers have been relatively consistent with standard models of flow and transport during a SWIW test.

The most striking difference compared with previous SWIW tests is that the rubidium curve shows a peak that is considerably higher than the Uranine curve. The Uranine curve (Figure 5-14a) appears somewhat noisy around the peak and the descending part appears to be almost a straight line rather than the typical declining tail of a tracer breakthrough curve.

The ascending part of the rubidium curve is slightly earlier than for cesium, which would indicate that rubidium would have stronger sorption capacity than cesium. On the other hand, the peak of the rubidium curve is much higher than for cesium, which would indicate the opposite.

The final tracer recoveries for the different tracers are difficult to estimate because the curves end well before the tailing parts have reached background values. Estimation of tracer recovery based on available experimental data result in values of 42.6% for Uranine, 53.9% for rubidium and 32.8% for cesium. These estimates are based on the average pumping flow rate during the recovery phase. The estimated recovery values are low compared with previous SWIW tests, at least for Uranine and cesium.

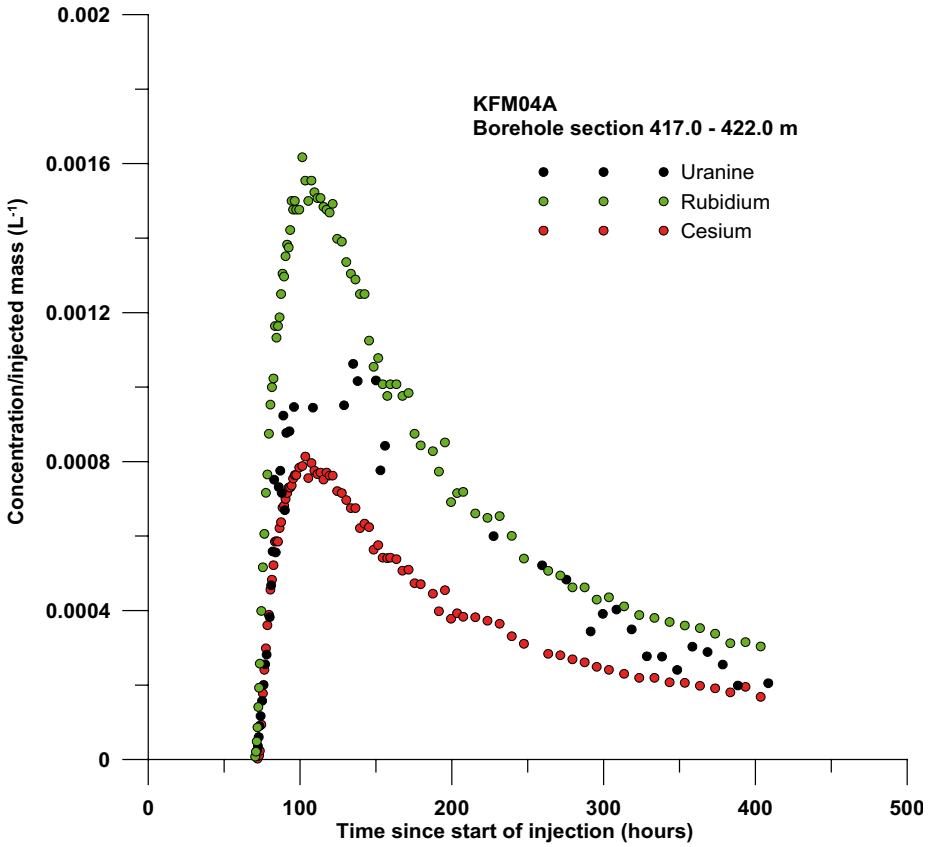


***Figure 5-15.*** *Normalised withdrawal (recovery) phase breakthrough curves for Uranine, cesium and rubidium in section 417.0–422.0 m.*

Final tracer recovery values, i.e. that would have resulted if pumping had been allowed to continue until tracer background values, are difficult to estimate from the experimental curves because of the unknown tailing parts. However, plausible extrapolations still result in fairly low tracer recovery. Even if one, hypothetically, also would extrapolate the peak of the uranine breakthrough curve (ignoring the seemingly noisy experimental values around the peak), tracer recovery would still likely not exceed 70%. Thus, it seems to be clear that a significant part of the injected Uranine is not recovered. Given that, in SWIW tests performed so far Uranine is typically fully recovered, a likely reason for incomplete recovery in this case might be that some of the injected water during the tracer injection and chaser injection phases is not recovered during the pumping phase. Instead, the "lost" tracer may have entered a larger fracture or fracture zone with a higher natural flow.

The tracer recovery for rubidium is the only value that may be considered not to be remarkably low. Plausible extrapolations of the tail do not exclude that rubidium might be close to fully recovered if pumping would continue. Cesium, on the other hand, seems to have a low recovery even if the tail would be extended. However, it may be possible that the cesium recovery is similar to the Uranine recovery.

### 5.2.3 Model evaluation KFM04A, 417.0–422.0 m

Due to the anomalous experimental data, as described above, a standard model evaluation (as described in Section 4.4.4) was difficult to carry out. Herein examples of two alternative interpretations of transport of Uranine and rubidium are presented. Attempts to model cesium were not successful due to the anomalous (late) ascending part of the breakthrough curve and the low recovery.

The model simulations involving Uranine and rubidium were carried out assuming negligible hydraulic background gradient, i.e. purely radial flow. From the dilution measurements, the ambient flow through the borehole section was estimated at about $9.6 \cdot 10^{-4}$ l/h, see Table 5-1, which is very small compared with the average flow rates during the SWIW test. The simulated times and flows for the various experimental phases are given in Table 5-2. This borehole section is interpreted to consist of 1–2 flowing fractures, see Table 4-2. In the simulation model, the flow zone is approximated by a 0.1 m thick fracture zone.

Figure 5-16 shows an example of simultaneous fitting of Uranine and rubidium, where all observation data are given equal regression weights. In this example, porosity, longitudinal dispersivity, and a retardation factor are included as regression parameters. Normally, porosity and dispersivity are linearly correlated and may not be estimated simultaneously from a SWIW test. However, in this case the porosity is allowed to vary in such a way that some of the injected tracer can leave the simulation model through the outer boundary, thereby simulating a loss to, for example, a nearby fracture zone. When used in this way, the porosity and dispersivity are not linearly correlated and may be estimated simultaneously.

Despite that the simulation models allow for some of the Uranine to "disappear", the model fit for Uranine is rather poor, as can be seen in Figure 5-16. One effect of letting some of the tracer disappear at the outer boundary is to make the Uranine recovery curve more narrow, making it more difficult to fit the tail, because the most remote part of the tracer is "cut off" at the end of the chaser injection period.

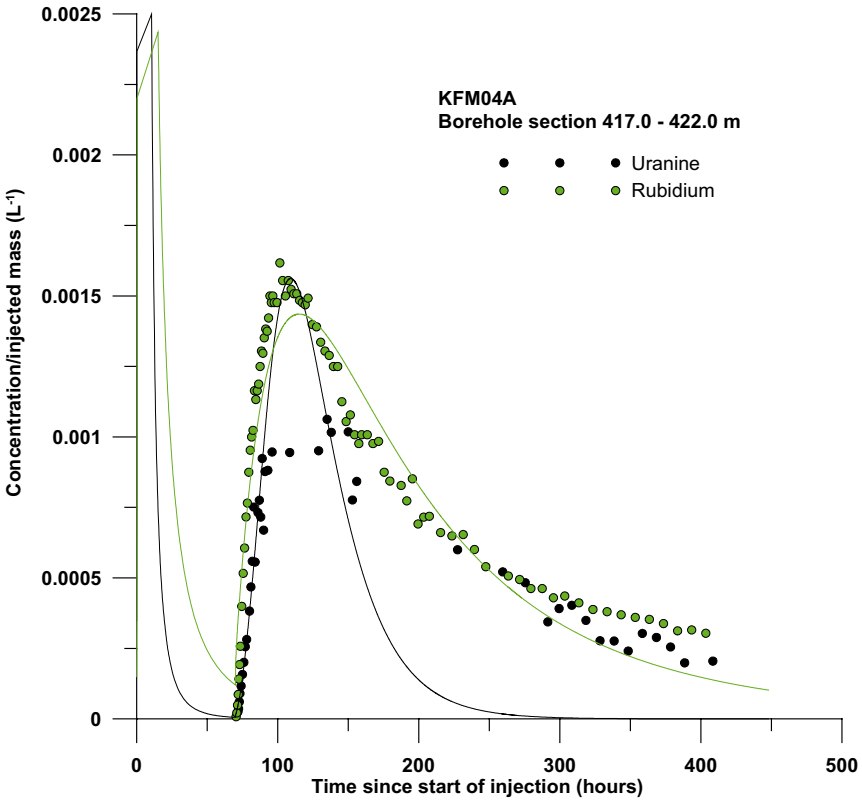


***Figure 5-16.*** *Example of simultaneous fitting of Uranine and rubidium for section 417.0–422.0 m in borehole KFM04A. All observation data are given equal regression weights.*

The second example presents an alternative interpretation where the seemingly noise observation data around the peak of the Uranine curve are excluded from the regression. In this case, tracer is not allowed to leave the simulation model. The result of this alternative interpretation is shown in Figure 5-17. The fit to the Uranine curve is quite different than in Figure 5-16, but whether one would consider this fit better or not seems to be a subjective choice. One may argue that the fitted curves in Figure 5-17 are more similar to the results in previous SWIW tests and that the tail for Uranine is closer to the observed one. The estimated retardation factor for rubidium is in this case 5.5 (R = 2.9 for the case in Figure 5-16). Considering the various anomalous features of the experimental data, these values of the retardation factor should be considered very uncertain. However, these results seem to indicate a moderate sorption effect for rubidium in this borehole section.

No attempts were made to determine a retardation factor for cesium because of the low recovery and otherwise apparently inconsistent features in the experimental breakthrough curve.

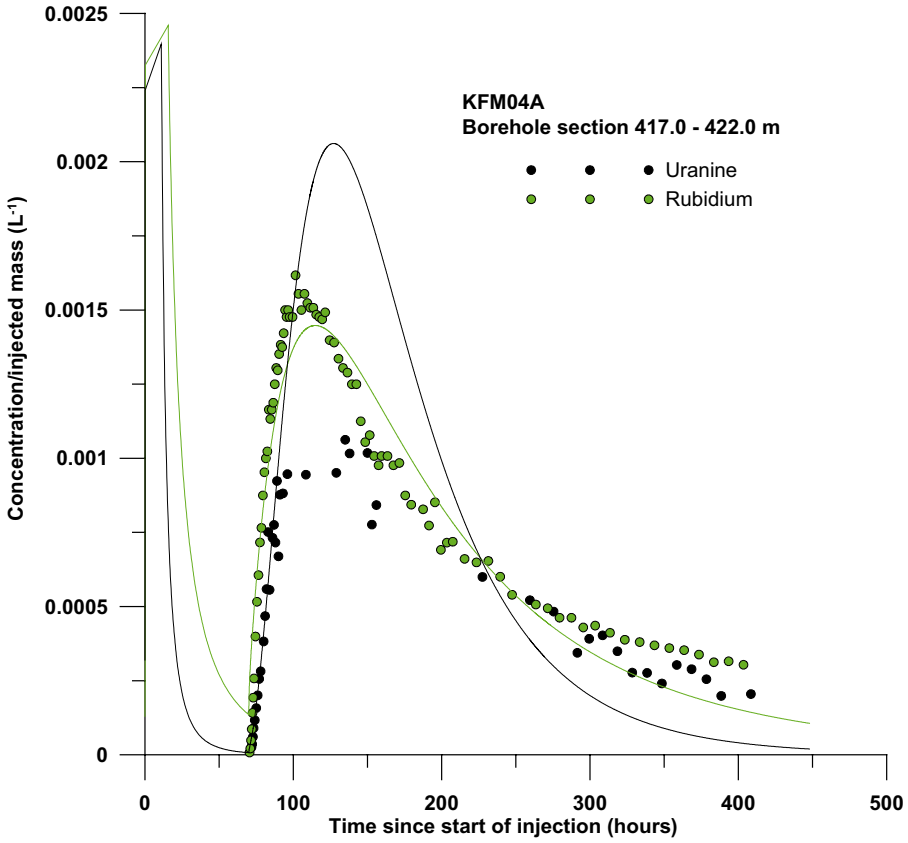


***Figure 5-17.*** *Example of simultaneous fitting of Uranine and rubidium for section 417.0–422.0 m in borehole KFM04A. Regression weights are assigned so that the seemingly noisy observation data around the peak of the Uranine curve are not included in the regression.*

# 6 Discussion and conclusions

The dilution measurements were carried out in selected fractures and fracture zones in borehole KFM04A at levels from 232 to 422 m borehole length (204 to 365 m vertical depth), where hydraulic transmissivity ranged within $T = 8.9 \cdot 10^{-9}$–$5.5 \cdot 10^{-5}$ m$^2$/s. The borehole intersects the deformation zones that are identified by SKB's single hole interpretation (SHI) of cored boreholes as seen in Figure 6-1 and as modelled in SDM version 2.1, Figure 6-2 and Table 6-1.

The results of the dilution measurements in borehole KFM04A show that the groundwater flow varies considerably during natural conditions, with flow rates from 0.004 to 16.6 ml/min and Darcy velocities from $3.5 \cdot 10^{-10}$ to $3.6 \cdot 10^{-7}$ m/s ($3.0 \cdot 10^{-5}$–$3.1 \cdot 10^{-2}$ m/d). These results are in accordance with dilution measurements carried out in boreholes KFM01A, KFM02A, KFM03A, KFM03B and KFM08A. In these boreholes hydraulic transmissivity in the test sections was within $T = 2.7 \cdot 10^{-10}$–$9.2 \cdot 10^{-5}$ m$^2$/s and flow rate ranged from 0.01 to 23.3 ml/min and Darcy velocity from $7.8 \cdot 10^{-10}$ to $8.4 \cdot 10^{-7}$ m/s ($6.7 \cdot 10^{-5}$–$7.3 \cdot 10^{-2}$ m/d) /Gustafsson et al. 2005, and Gustafsson et al. 2006b/.

Groundwater flow rates and Darcy velocities calculated from dilution measurements in borehole KFM04A are also within the range that can be expected out of experience from previously preformed dilution measurements under natural gradient conditions at other sites in Swedish crystalline rock /Gustafsson and Andersson 1991, Gustafsson and Morosini 2002, Gustafsson and Nordqvist 2005, and /Gustafsson et al. 2006a/. In KFM04A The highest flow rate and Darcy velocity is measured in the upper part of the deformation zone ZFMNE00A2 at 232–237 m borehole length (204.0–208.3 m vertical depth).The lowest flow rate is measured in the low transmissive single fracture at c. 296 m borehole length (260 m vertical depth) and the lowest Darcy velocity is measured in the deformation zone ZFMNE1188 at 417–422 m borehole length (361.0–365.1 m vertical depth). The determined groundwater flow rates are fairly proportional to the hydraulic transmissivity, although the statistical basis is weak.

**Table 6-1. Intersected zones, groundwater flow rates, Darcy velocities and hydraulic gradients for all measured sections in boreholes KFM04A.**

| Borehole | Test section (m)+ | Intersected zones*** | Number of flowing fractures* | T (m$^2$/s) | Q (ml/min) | Q (m$^3$/s) | Darcy velocity (m/s) | Hydraulic gradient |
|---|---|---|---|---|---|---|---|---|
| KFM04A | 232.0–237.0 (204.0–208.3) | DZ3/ ZFMNE00A2 | 3 | 5.50E–05* | 16.618 | 2.77E–07 | 3.60E–07 | 0.033 |
| KFM04A | 296.5–297.5 (259.5–260.3) | | 1 | 1.61E–07* | 0.004 | 7.06E–11 | 4.58E–10 | 0.003 |
| KFM04A | 359.3–360.3 (312.9–313.7) | | 1 | 1.26E–06* | 0.955 | 1.59E–08 | 1.03E–07 | 0.082 |
| KFM04A | 417.0–422.0 (361.0–365.1) | DZ4/ ZFMNE1188 | 1–2 | 8.91E–09** | 0.016 | 2.72E–10 | 3.54E–10 | 0.198 |

* /Rouhiainen and Pöllänen 2004/.

** /Hjerne and Ludvigson 2005/.

*** /SKB 2006/.

+ Test section vertical depth is given within brackets.

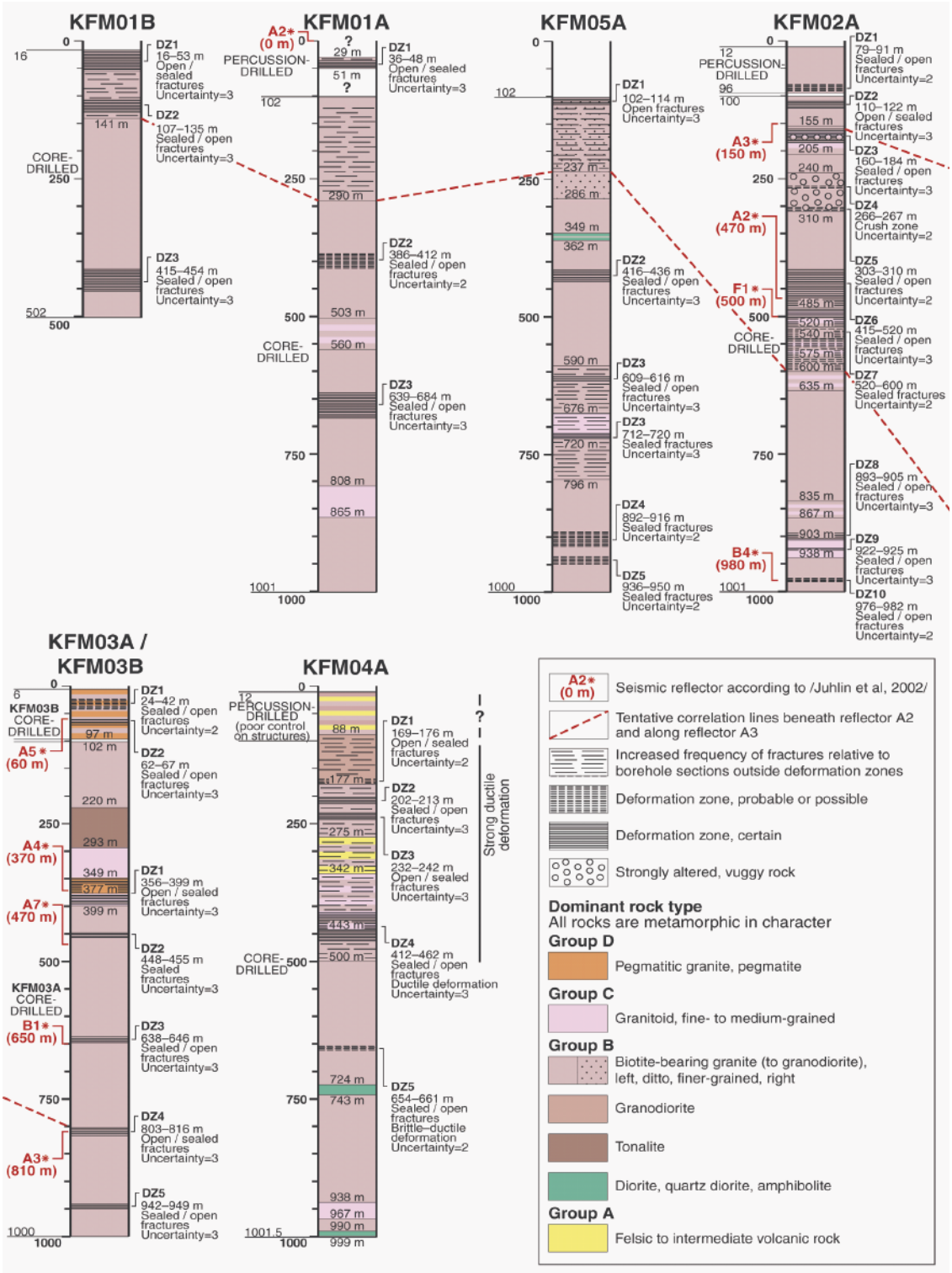


***Figure 6-1.*** *Rock units and possible deformation zones in the cored boreholes based on the single hole interpretations. (From /SKB 2005/, Figure 5-48).*

Hydraulic gradients in KFM04A, calculated according to the Darcy concept, are within the expected range (0.001–0.05) in two out of four measured test sections. In the single fracture section at c. 359 m (313 m vertical depth) and in the fracture zone at c. 417 m borehole length (361 m vertical depth) the hydraulic gradient is considered to be large. Local effects where the measured fractures constitute a hydraulic conductor between other fractures with different hydraulic heads or wrong estimations of the correction factor, α, and/or the hydraulic

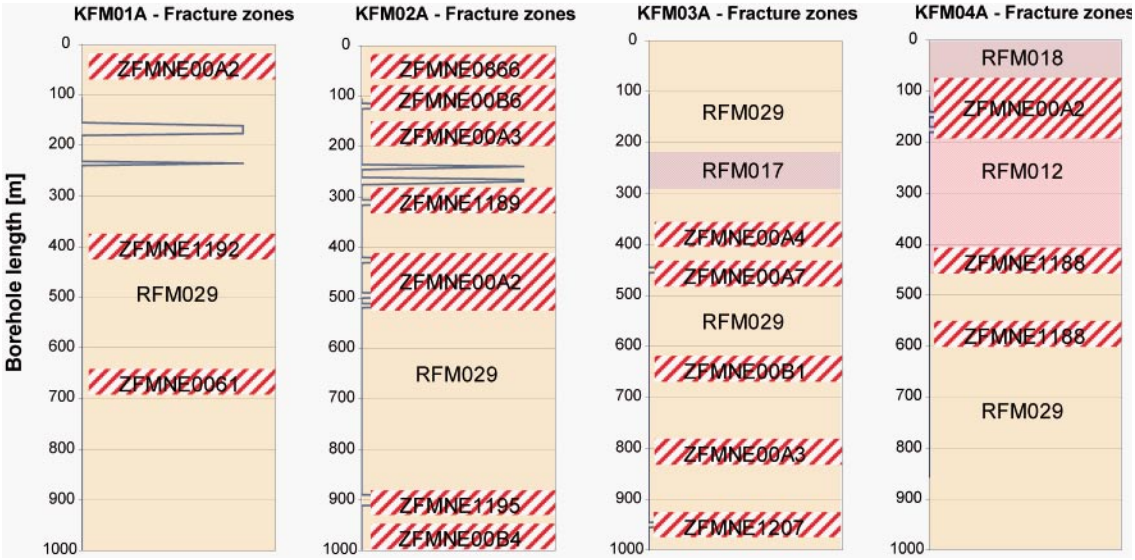


***Figure 6-2.*** *Plot of the minor deformation zones identified by means of the empirical methods Q and RMS along the boreholes (Q < 10 and/or RMS < 65). The deterministic deformation zones in version 1.2 are also indicated. (From /SKB 2006/).*

conductivity of the fracture could explain the large hydraulic gradients. The pressure decrease at the beginning of the measurement and the clogging of the optical device at c. 417 m may give some contribution to the measured groundwater flow rate and hence to the large calculated hydraulic gradient. The hydraulic transmissivity of the section is at lower limit of measurement range for the dilution probe which may decrease accuracy in determined groundwater flow rate.

The SWIW experiments in the borehole section described here resulted in relatively anomalous tracer breakthrough data, compared with previous tests within the site investigation programmes. Several unusual features in the collected data made a standard model evaluation difficult, particularly for cesium for which no model evaluation is presented in this report. Two examples of evaluation of Uranine and rubidium are presented, although evaluated data from these should be considered very uncertain.

The anomalous features in the experimental data include low tracer recovery, especially for Uranine and cesium. In addition, normalised cesium breakthrough data give an ambiguous impression as the ascending part indicates very little sorption (cesium has shown to be strongly sorbing in all previous SWIW tests within the site investigation programmes), while the remainder of the curve is more consistent with a strongly sorbing tracer.

One may speculate that the low recovery for Uranine is caused by irreversible tracer losses during the water injection phases by pushing the tracer out into other, with higher ambient flow, fractures or fracture zones. However, model simulations indicate that this would sharpen the peak of the recovery curve which would actually make it still more difficult to fit the model to the data. An alternative hypothesis might be that the injected water spreads in several more or less independent flow paths. Then it might be possible that some of the non-sorbing tracer (Uranine) is irreversibly lost in one or a few of the flow paths, but this does not happen, to the same extent, to the more strongly sorbing tracers. This would, however, still not explain the low recovery and otherwise anomalous behaviour of cesium.

From the example model simulations, the estimated retardation factor for rubidium is in the interval of 2.9 to 5.5. However, these values should be considered as very uncertain. Estimated retardation factors from previous SWIW tests /Gustafsson et al. 2006ab/ have been significantly higher.

# 7 References


**Andersson P, 1995.** Compilation of tracer tests in fractured rock. SKB PR 25-95-05, Svensk Kärnbränslehantering AB.

**Andersson P, Byegård J, Winberg A, 2002.** Final report of the TRUE Block Scale project. 2. Tracer tests in the block scale. SKB TR-02-14, Svensk Kärnbränslehantering AB.

**Byegård J, Tullborg E-L, 2005.** Sorption experiments and leaching studies using fault gouge material and rim zone material from the Äspö Hard Rock Laboratory. SKB Technical Report (in prep.).

**Gustafsson E, 2002.** Bestämning av grundvattenflödet med utspädningsteknik – Modifiering av utrustning och kompletterande mätningar. SKB R-02-31 (in Swedish), Svensk Kärnbränslehantering AB.

**Gustafsson E, Andersson P, 1991.** Groundwater flow conditions in a low-angle fracture zone at Finnsjön, Sweden. Journal of Hydrology, Vol 126, pp 79–111. Elsvier, Amsterdam.

**Gustafsson E, Morosini M, 2002.** In situ groundwater flow measurements as a tool for hardrock site characterisation within the SKB programme. Norges geologiske undersøkelse. Bulletin 439, 33–44.

**Gustafsson E, Nordqvist R, 2005.** Oskarshamn site investigation. Groundwater flow measurements and SWIW-tests in boreholes KLX02 and KSH02. SKB P-05-28, Svensk Kärnbränslehantering AB.

**Gustafsson E, Nordqvist R, Thur P, 2005.** Forsmark site investigation. Groundwater flow measurements and SWIW tests in boreholes KFM01A, KFM02A, KFM03A and KFM03B. SKB P-05-77, Svensk Kärnbränslehantering AB.

**Gustafsson E, Nordqvist R, Thur P, 2006a.** Oskarshamn site investigation. Groundwater flow measurements and SWIW-tests in borehole KLX03. SKB P-05-246, Svensk Kärnbränslehantering AB.

**Gustafsson E, Nordqvist R, Thur P, 2006b.** Forsmark site investigation. Groundwater flow measurements and SWIW tests in borehole KFM08A. SKB P-06-90, Svensk Kärnbränslehantering AB.

**Halevy E, Moser H, Zellhofer O, Zuber A, 1967.** Borehole dilution techniques – a critical review. In: Isotopes in Hydrology, Proceedings of a Symposium, Vienna 1967, IAEA, Vienna, pp 530–564.

**Hjerne C, Ludvigson J-E, 2005.** Forsmark site investigation. Single-hole injection tests in borehole KFM04A. SKB P-04-293, Svensk Kärnbränslehantering AB.

**Nordqvist R, Gustafsson E, 2004.** Single-well injection-withdrawal tests (SWIW). Investigation of evaluation aspects under heterogeneous crystalline bedrock conditions. SKB R-04-57, Svensk Kärnbränslehantering AB.

**Rhén I, Forsmark T, Gustafson G, 1991.** Transformation of dilution rates in borehole sections to groundwater flow in the bedrock. Technical note 30. In: Liedholm M. (ed) 1991. SKB-Äspö Hard Rock Laboratory, Conceptual Modeling of Äspö, technical Notes 13–32. General Geological, Hydrogeological and Hydrochemical information. Äspö Hard Rock Laboratory Progress Report PR 25-90-16b, Svensk Kärnbränslehantering AB.

**Rouhiainen P, Pöllänen J, 2004.** Forsmark site investigation. Difference flow logging in borehole KFM04A. SKB P-04-190, Svensk Kärnbränslehantering AB.

**SKB, 2001a.** Program för platsundersökning vid Forsmark. SKB R-01-42 (in Swedish), Svensk Kärnbränslehantering AB.

**SKB, 2001b.** Site investigations – Investigation methods and general execution programme. SKB TR-01-29, Svensk Kärnbränslehantering AB.

**SKB, 2005.** Preliminary site description. Forsmark area – version 1.2. SKB R-05-18, Svensk Kärnbränslehantering AB.

**SKB, 2006.** Site modelling Forsmark step 2.1. SKB R-06-38, Svensk Kärnbränslehantering AB.

**Voss C I, 1984.** SUTRA – Saturated-Unsaturated Transport. A finite element simulation model for saturated-unsaturated fluid-density-dependent groundwater flow with energy transport or chemically-reactive single-species solute transport. U.S. Geological Survey Water-Resources Investigations Report 84-4369.

# Appendix A

## Borehole data KFM04A

### SICADA – Information about KFM04A

| Title | Value<br>Information about cored borehole KFM04A (2006-06-27). | | | | |
|---|---|---|---|---|---|
| **Borehole length (m):** | 1001.420 | | | | |
| **Reference level:** | Fläns casing | | | | |
| **Drilling period(s):** | From date | To date | Secup (m) | Seclow (m) | Drilling type |
| | 2003-05-20 | 2003-06-30 | 0.000 | 107.420 | Percussion drilling |
| | 2003-08-25 | 2003-11-19 | 107.420 | 1,001.420 | Core drilling |
| **Starting point coordinate:** | Length (m) | Northing (m) | Easting (m) | Elevation | Coord system |
| | 0.000 | 6698921.744 | 1630978.964 | 8.771 | RT90-RHB70 |
| **Angles:** | Length (m) | Bearing | Inclination (– = down) | Coord system | |
| | 0.000 | 45.244 | –60.081 | RT90-RHB70 | |
| **Borehole diameter:** | Secup (m) | Seclow (m) | Hole diam (m) | | |
| | 0.000 | 12.030 | 0.350 | | |
| | 12.030 | 107.330 | 0.247 | | |
| | 107.330 | 107.420 | 0.161 | | |
| | 107.420 | 108.690 | 0.086 | | |
| | 108.690 | 1,001.420 | 0.077 | | |
| **Core diameter:** | Secup (m) | Seclow (m) | Core diam (m) | | |
| | 107.420 | 108.690 | 0.072 | | |
| | 108.690 | 1,000.890 | 0.051 | | |
| | 1,000.890 | 1,001.420 | 0.062 | | |
| **Casing diameter:** | Secup (m) | Seclow (m) | Case in (m) | Case out (m) | Comment |
| | 0.000 | 106.910 | 0.200 | 0.208 | |
| | 0.000 | 12.030 | 0.265 | 0.273 | |
| | 0.000 | 12.030 | 0.265 | 0.273 | |
| | 0.000 | 106.910 | 0.200 | 0.208 | |
| | 106.910 | 106.950 | 0.170 | 0.208 | |
| | 106.910 | 106.950 | 0.170 | 0.208 | |
| **Grove milling:** | Length (m) | Trace detectable | | | |
| | 119.000 | 119 | | | |
| | 150.000 | 150 | | | |
| | 200.000 | 199 | | | |
| | 250.000 | 250 | | | |
| | 300.000 | 300 | | | |
| | 350.000 | 349 | | | |
| | 400.000 | 400 | | | |
| | 450.000 | 449 | | | |
| | 500.000 | 500 | | | |
| | 550.000 | 550 | | | |
| | 600.000 | 600 | | | |
| | 650.000 | 650 | | | |
| | 700.000 | 700 | | | |
| | 750.000 | 750 | | | |
| | 800.000 | 800 | | | |
| | 850.000 | 850 | | | |
| | 900.000 | 900 | | | |
| | 950.000 | 950 | | | |
| **Installed sections:** | Section no | Start date | Secup (m) | Seclow (m) | |
| | 1 | 2004-06-30 | 0.000 | 1,001.420 | |

## Dilution measurement KFM04A 232.0–237.0 m

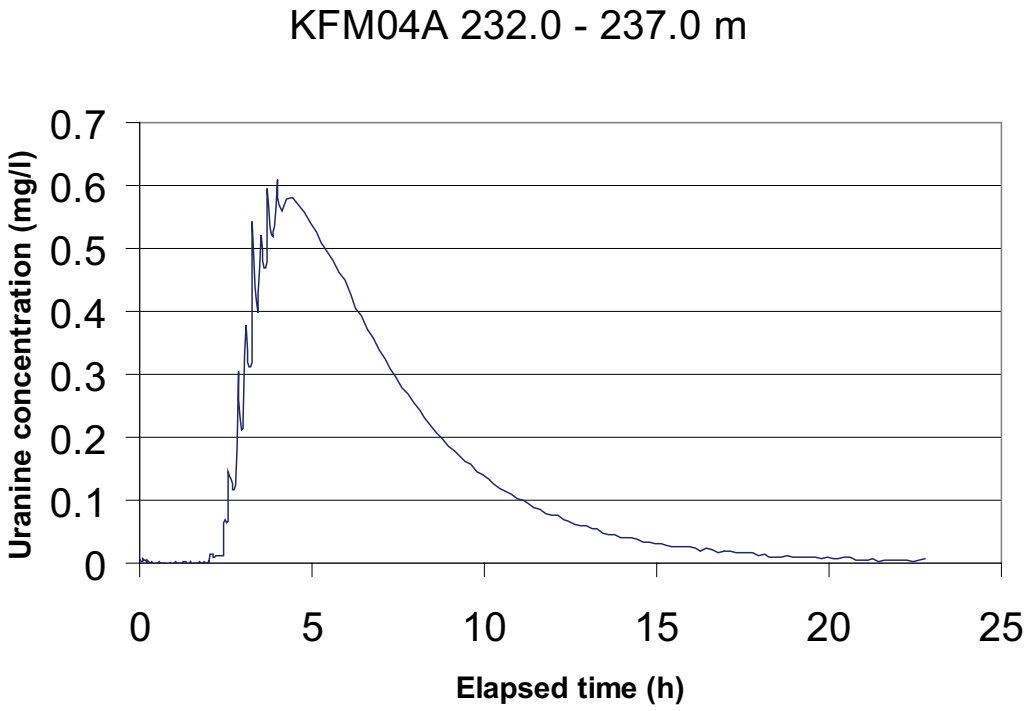


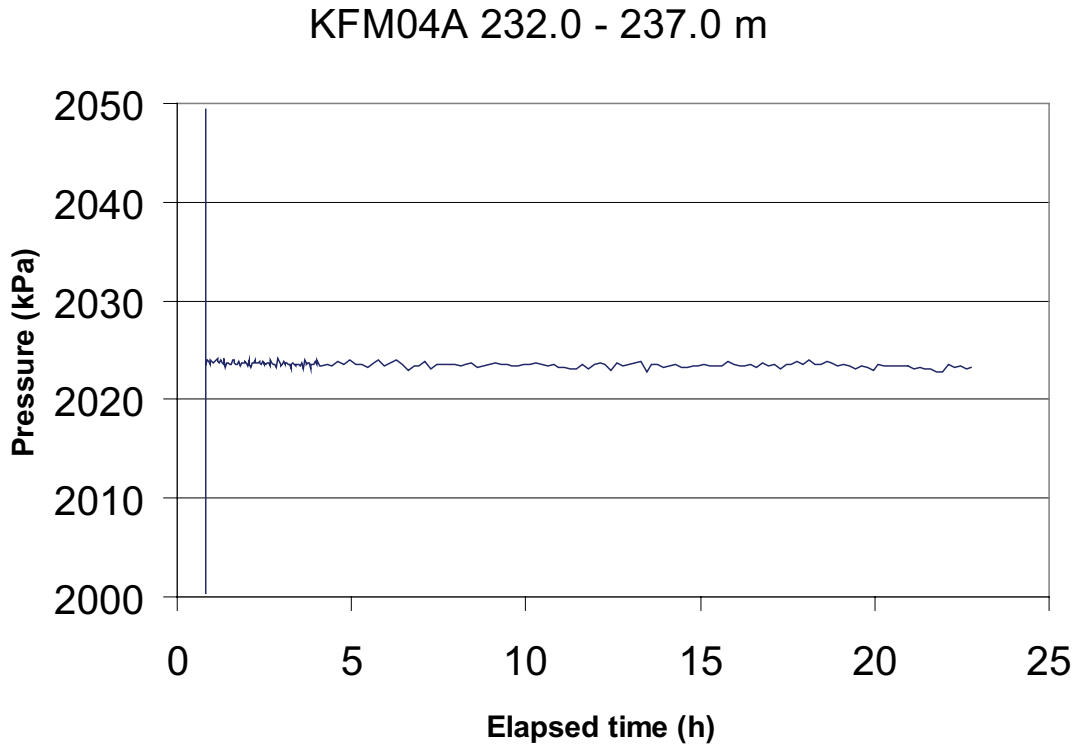

KFM04A 232.0 - 237.0 m

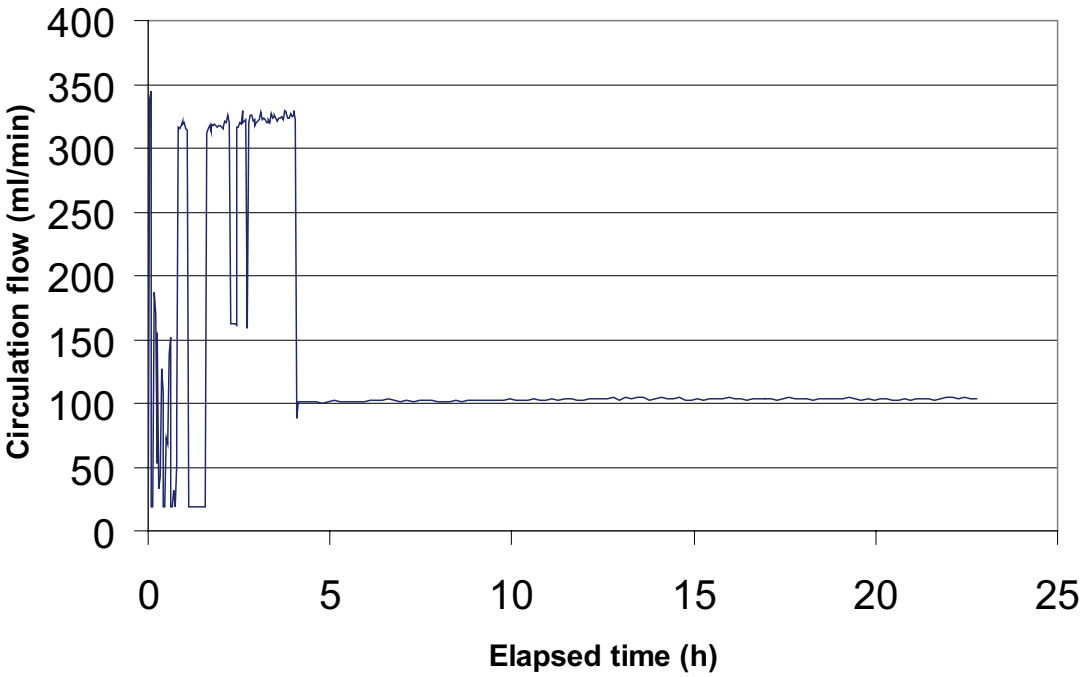


KFM04A 232.0 - 237.0 m

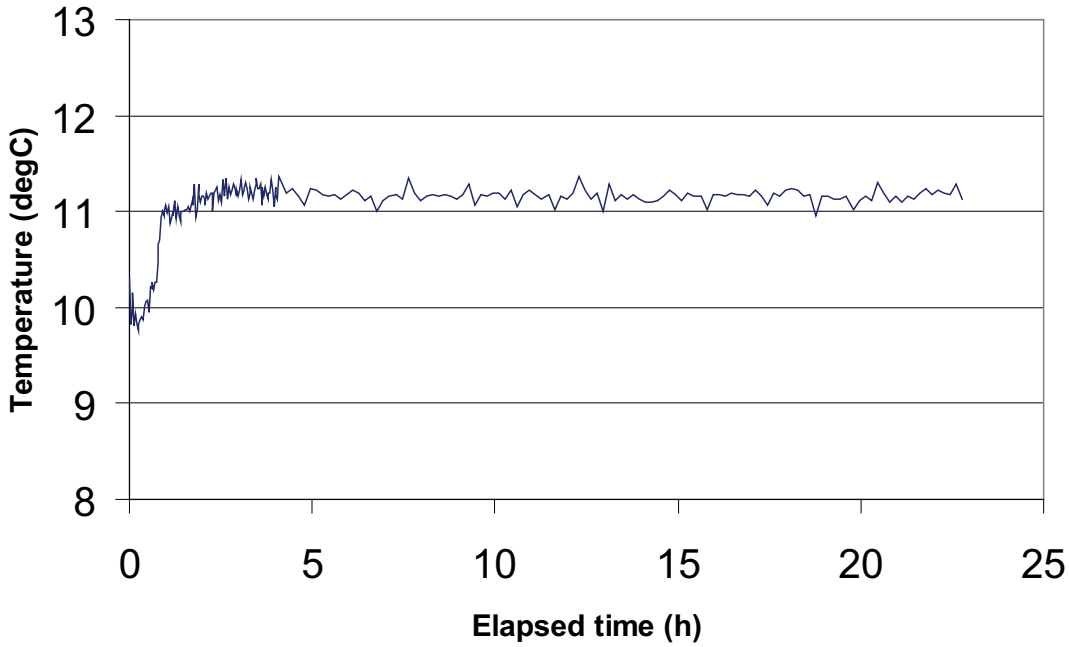

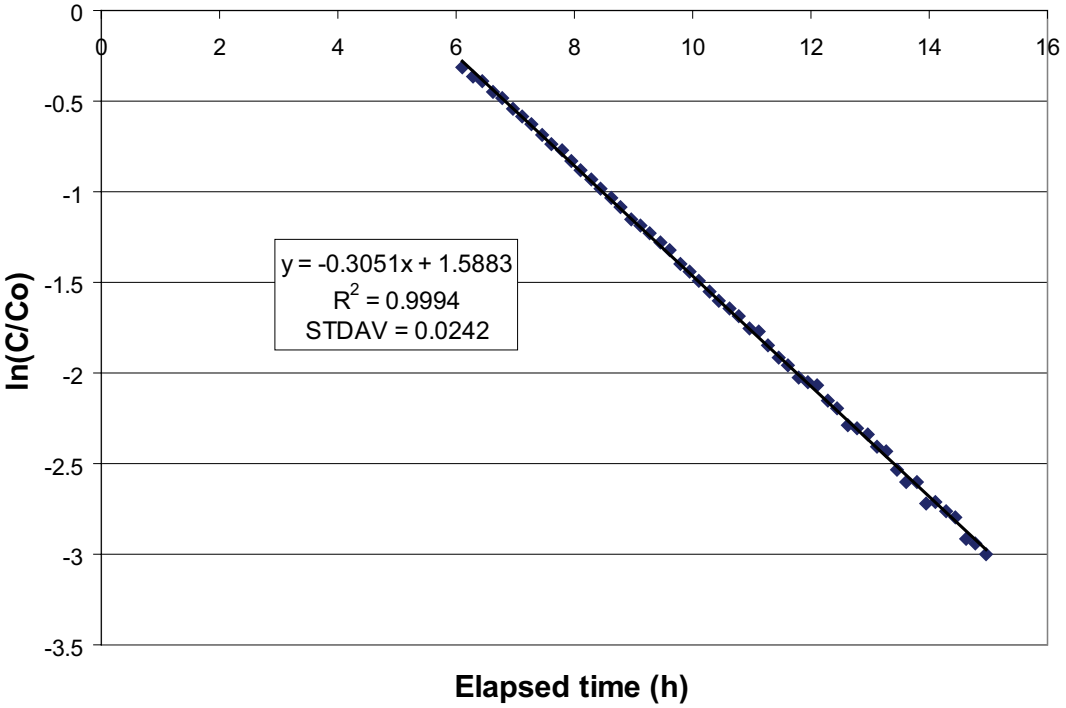


| Part of dilution curve (h) | V (ml) | ln(C/Co)/t | Q (ml/h) | Q (ml/min) | Q (m3/s) | R2-value |
|---|---|---|---|---|---|---|
| 6 ~15 | 3268 | -0.3051 | 997.07 | 16.618 | 2.77E-07 | 0.9994 |

| Part of dilution curve (h) | K (m/s) | Q (m3/s) | A (m2) | v(m/s) | I |
|---|---|---|---|---|---|
| 6 ~15 | 1.10E-05 | 2.77E-07 | 0.7700 | 3.60E-07 | 0.033 |

## Dilution measurement KFM04A 296.5–297.5 m

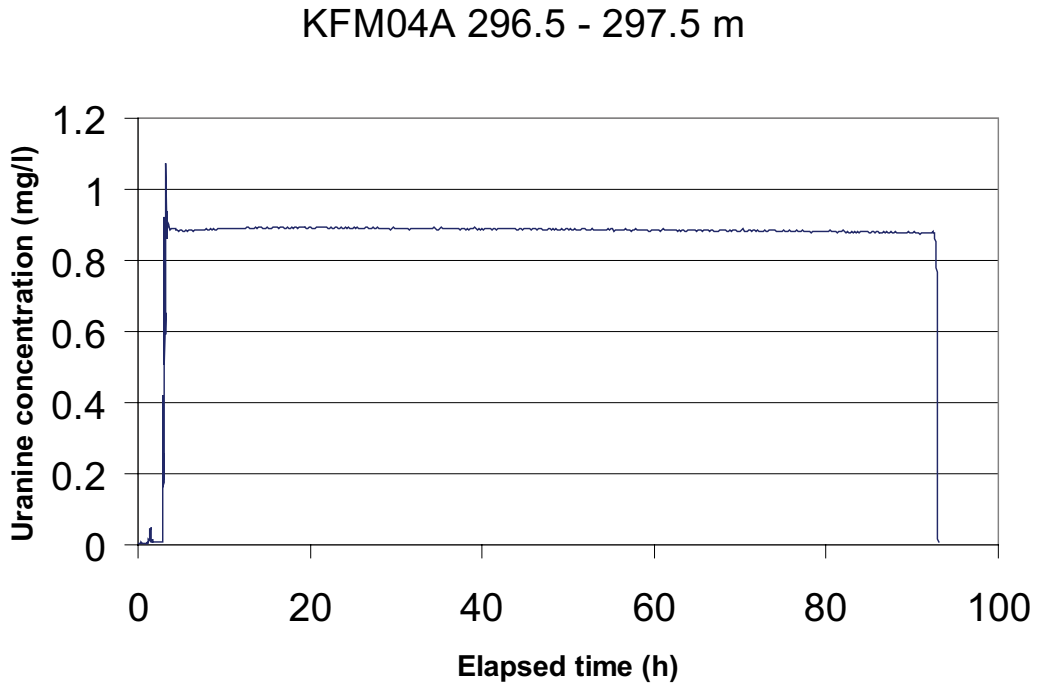


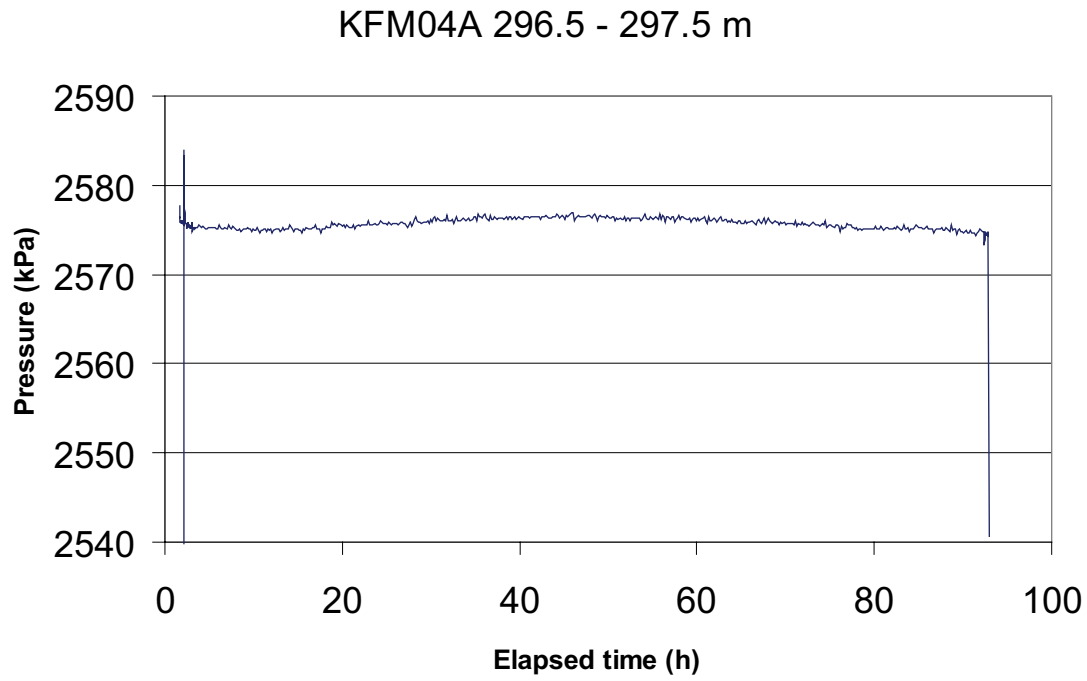

KFM04A 296.5 - 297.5 m

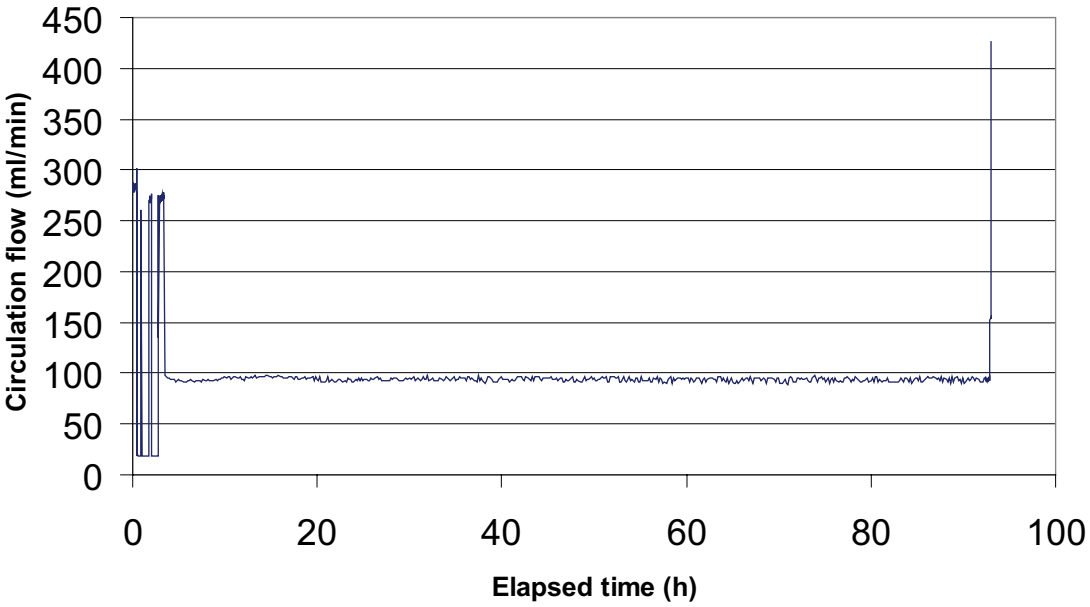


KFM04A 296.5 - 297.5 m

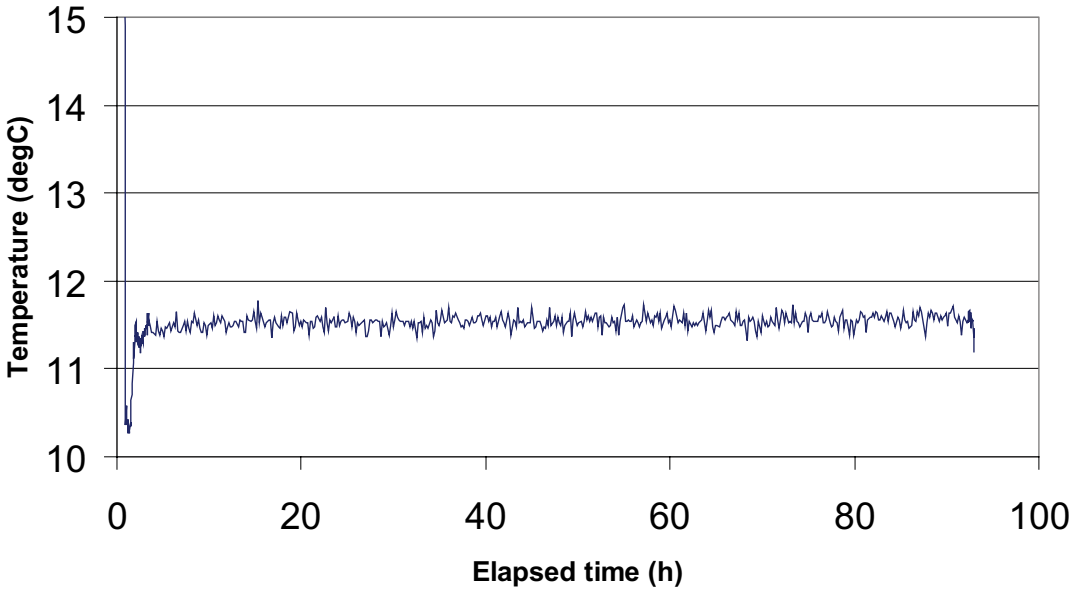

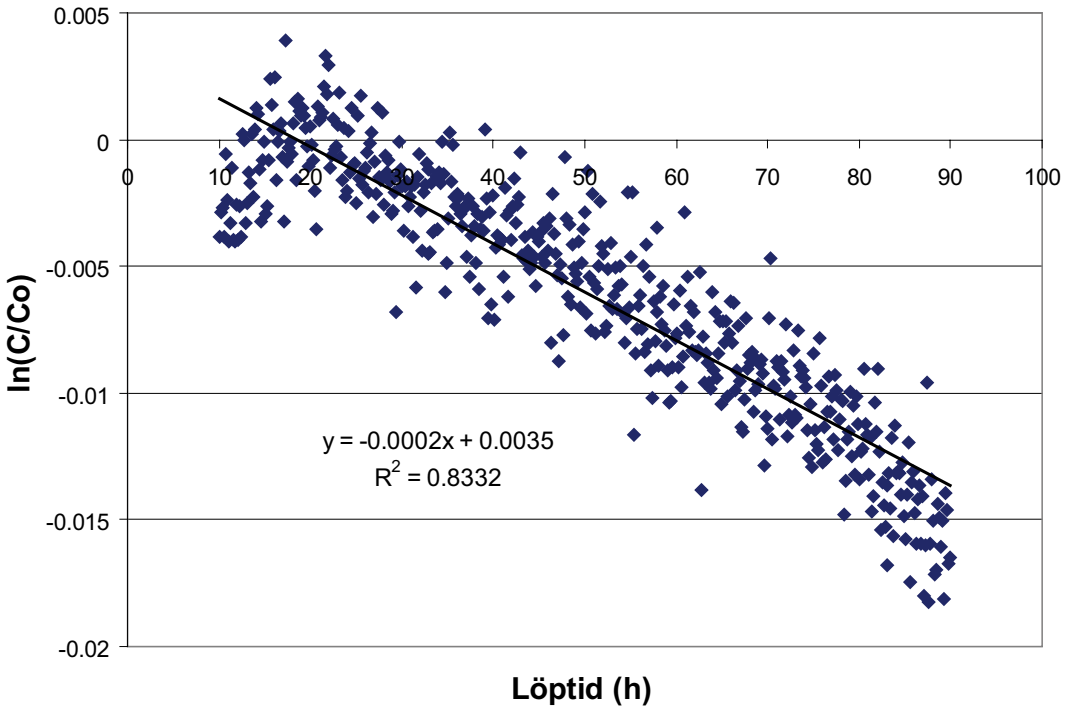


| Part of dilution curve (h) | V (ml) | ln(C/Co)/t | Q (ml/h) | Q (ml/min) | Q (m3/s) | R2-value |
|---|---|---|---|---|---|---|
| 10-90 | 1270 | -0.0002 | 0.25 | 0.004 | 7.06E-11 | 0.8332 |

| Part of dilution curve (h) | K (m/s) | Q (m3/s) | A (m2) | v(m/s) | I |
|---|---|---|---|---|---|
| 10-90 | 1.61E-07 | 7.06E-11 | 0.1540 | 4.58E-10 | 0.003 |

## Dilution measurement KFM04A 359.3–360.3 m

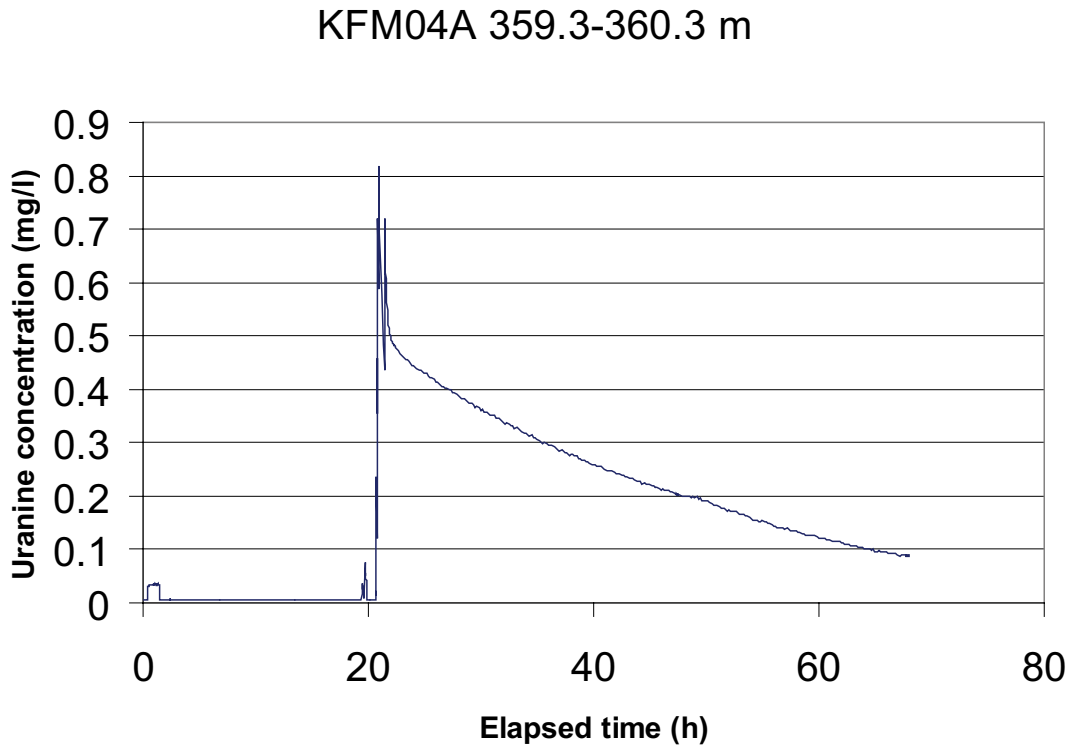


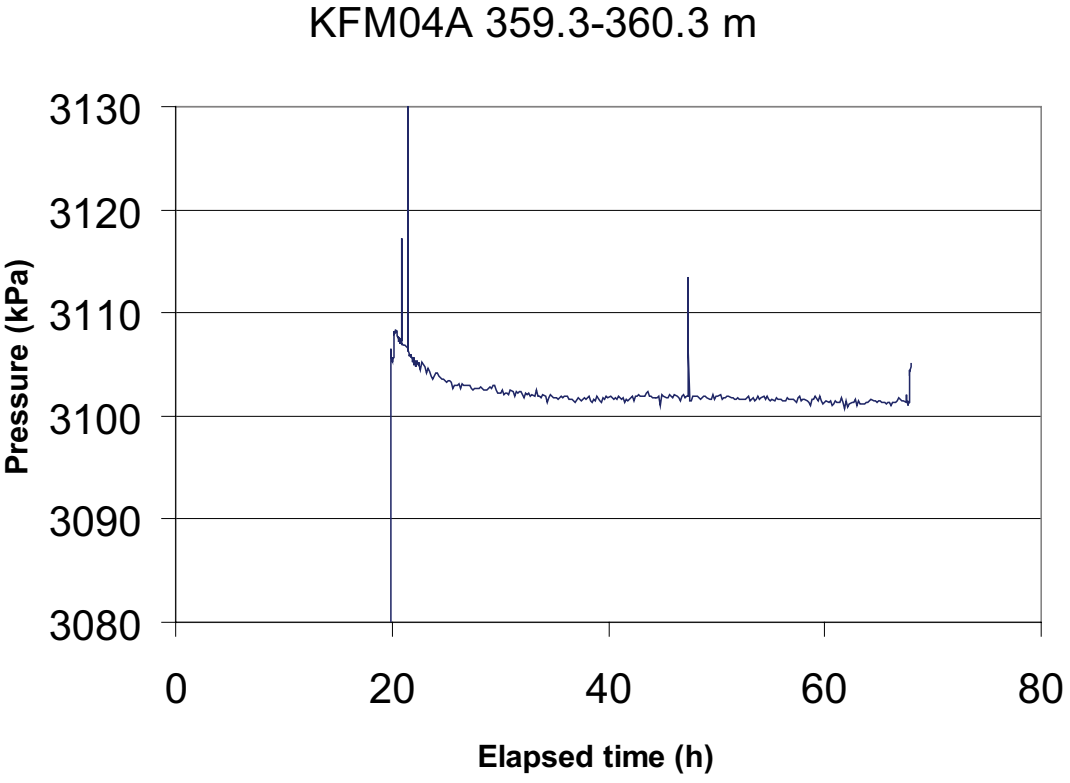

KFM04A 359.3-360.3 m

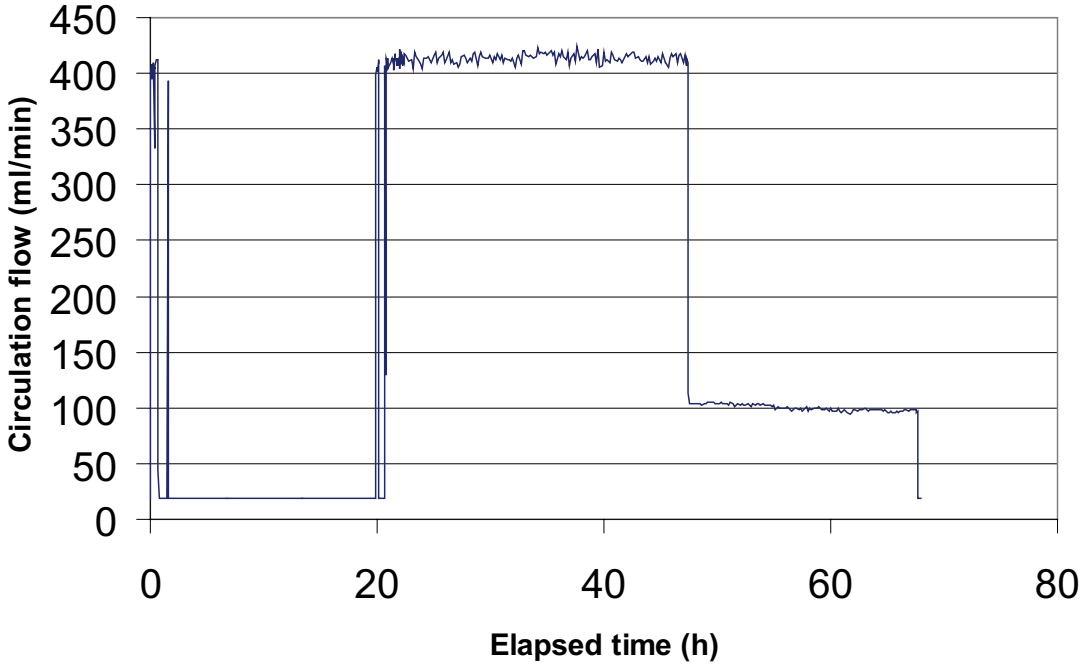


KFM04A 359.3-360.3 m

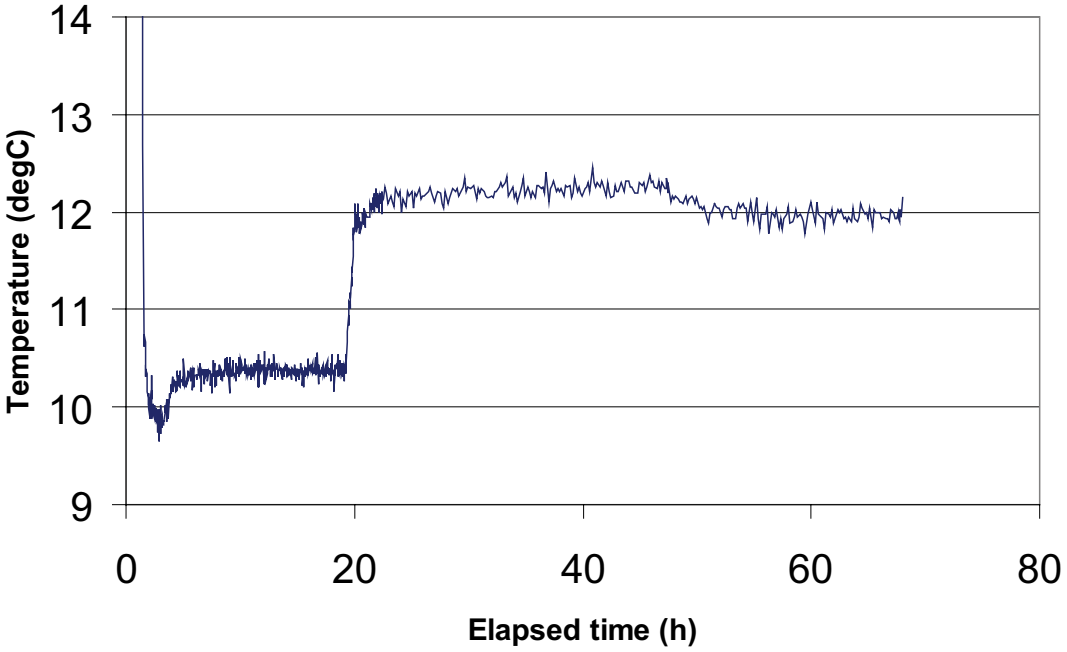

KFM04A 359.3-360.3 m

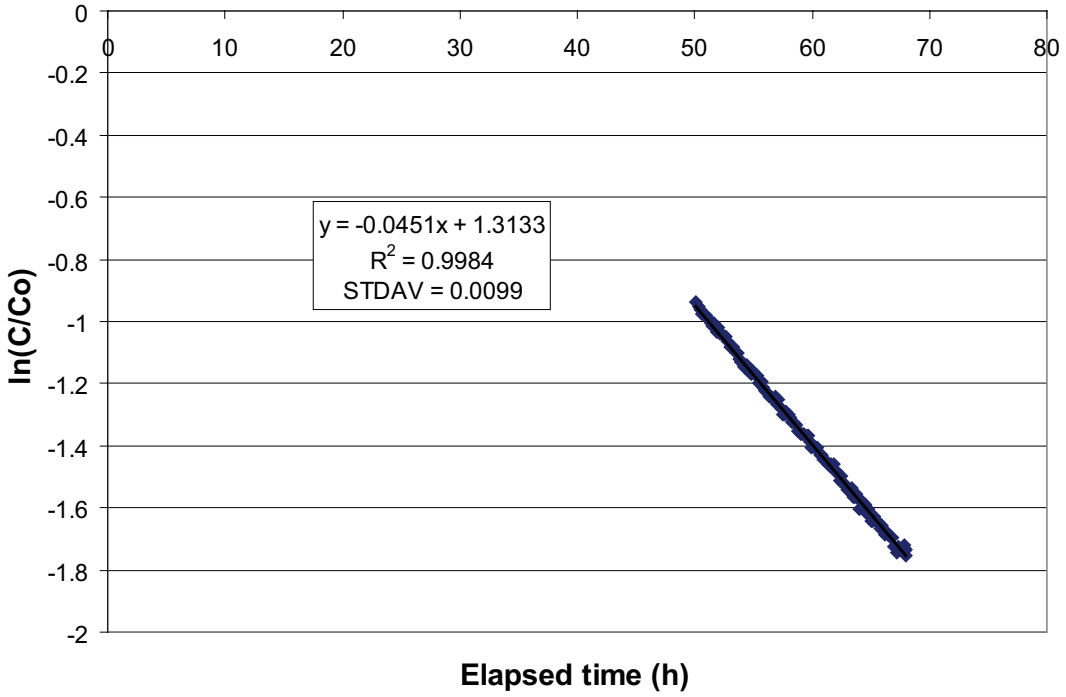


| Part of dilution curve (h) | V (ml) | ln(C/Co)/t | Q (ml/h) | Q (ml/min) | Q (m3/s) | R2-value |
|---|---|---|---|---|---|---|
| 50-67 | 1270 | -0.0451 | 57.28 | 0.955 | 1.59E-08 | 0.9984 |

| Part of dilution curve (h) | K (m/s) | Q (m3/s) | A (m2) | v(m/s) | I |
|---|---|---|---|---|---|
| 50-67 | 1.26E-06 | 1.59E-08 | 0.1540 | 1.03E-07 | 0.082 |

## Dilution measurement KFM04A 417.0–422.0 m

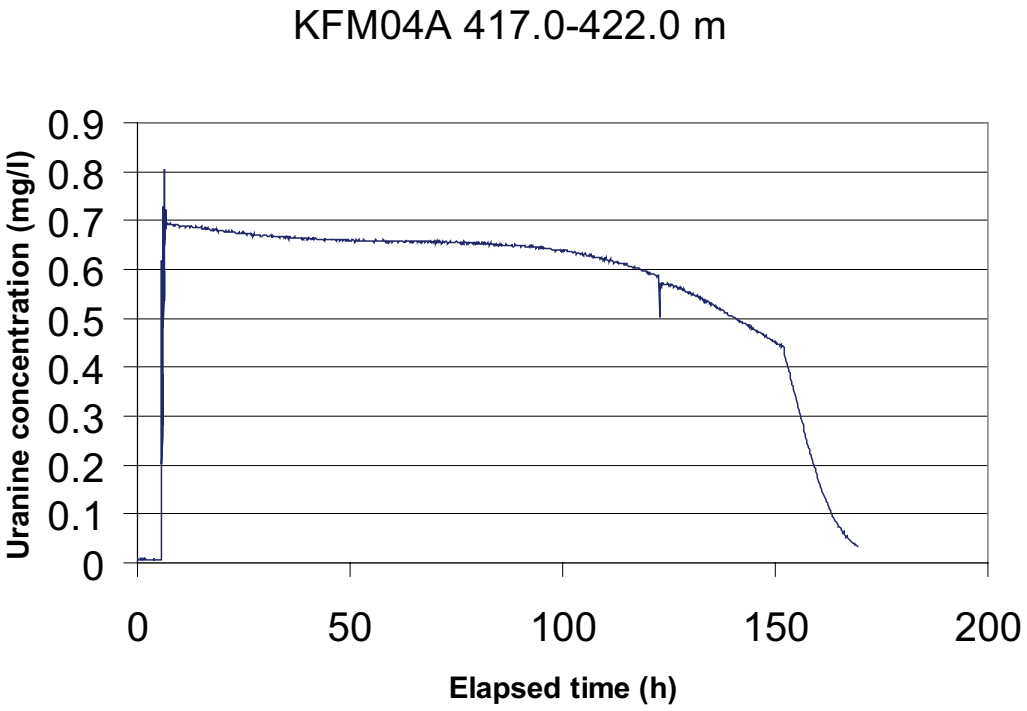


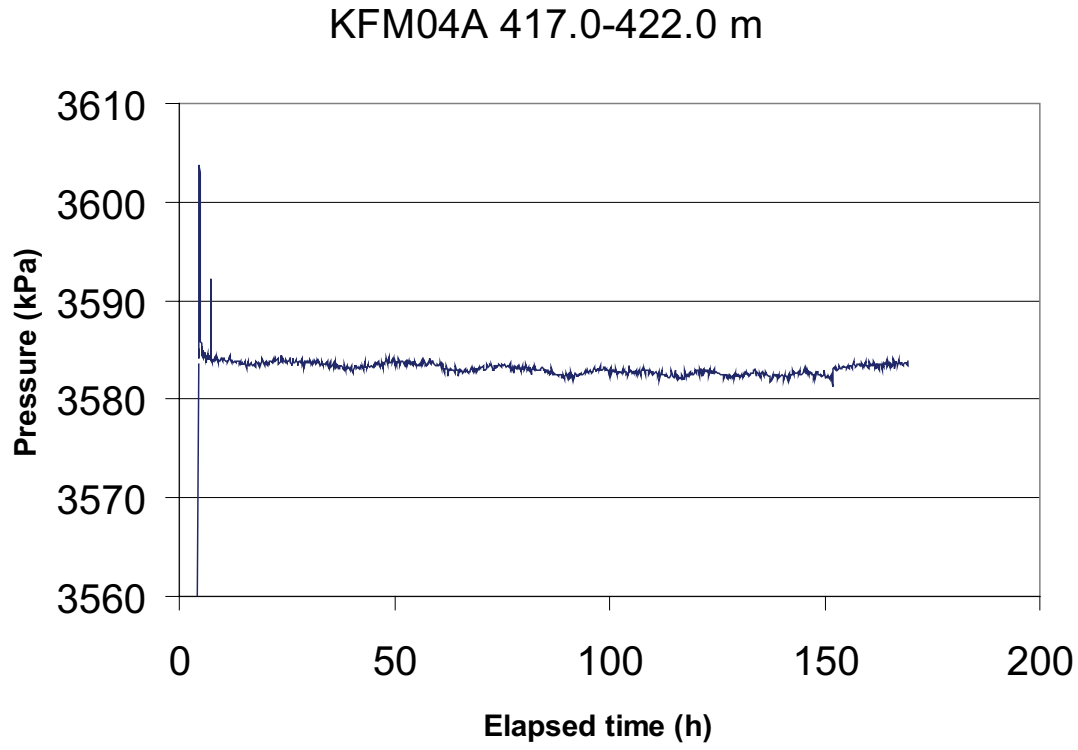

KFM04A 417.0-422.0 m

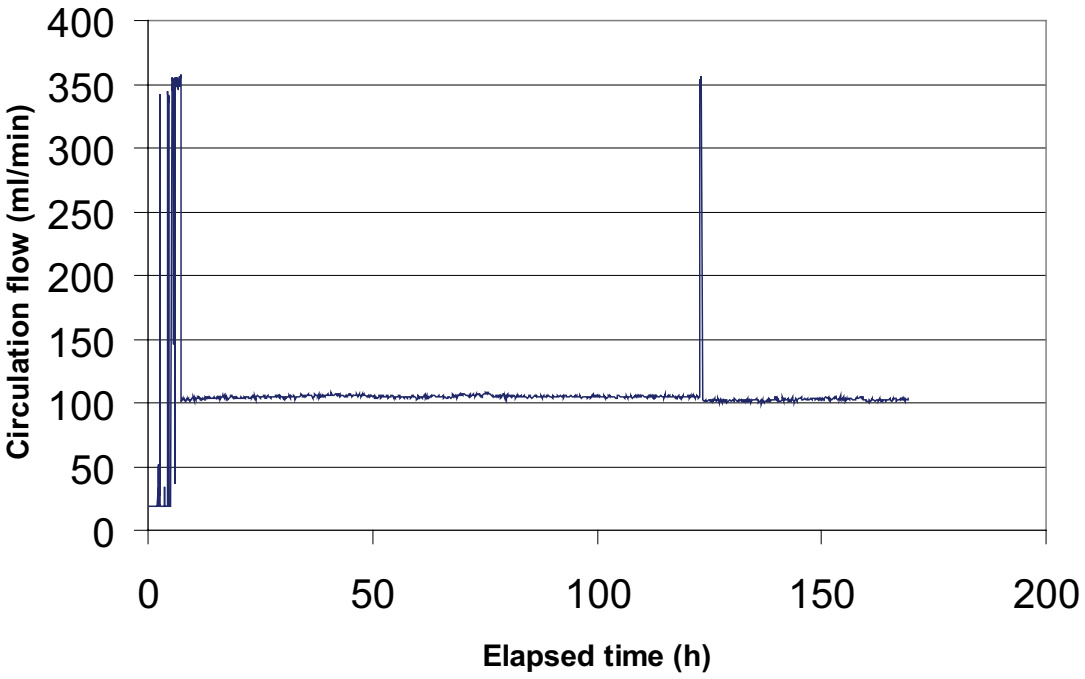


KFM04A 417.0-422.0 m

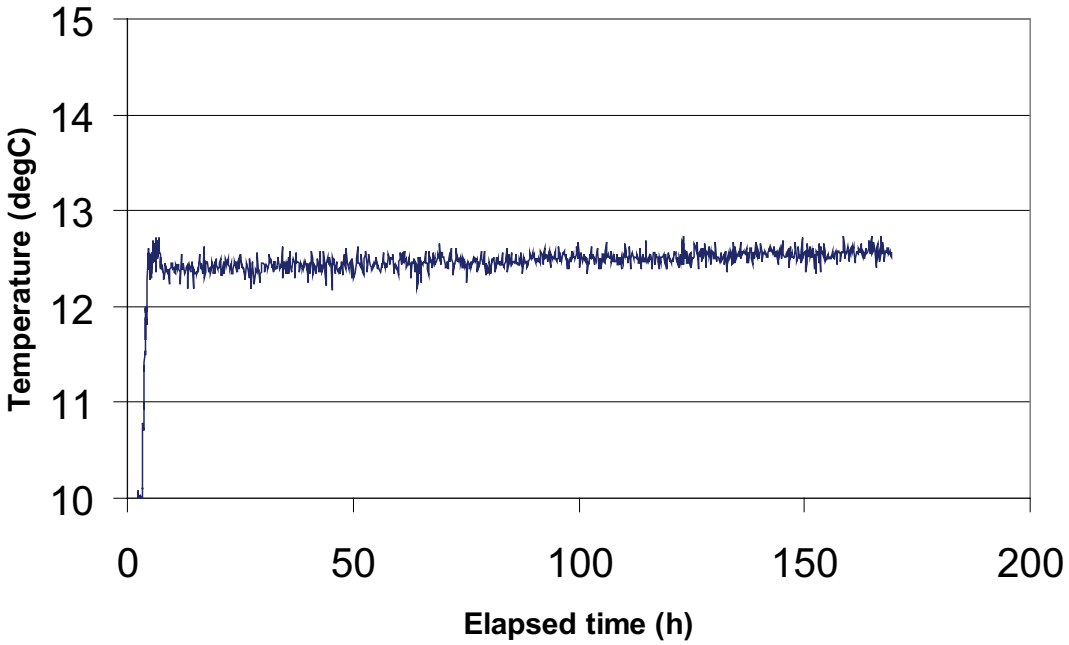

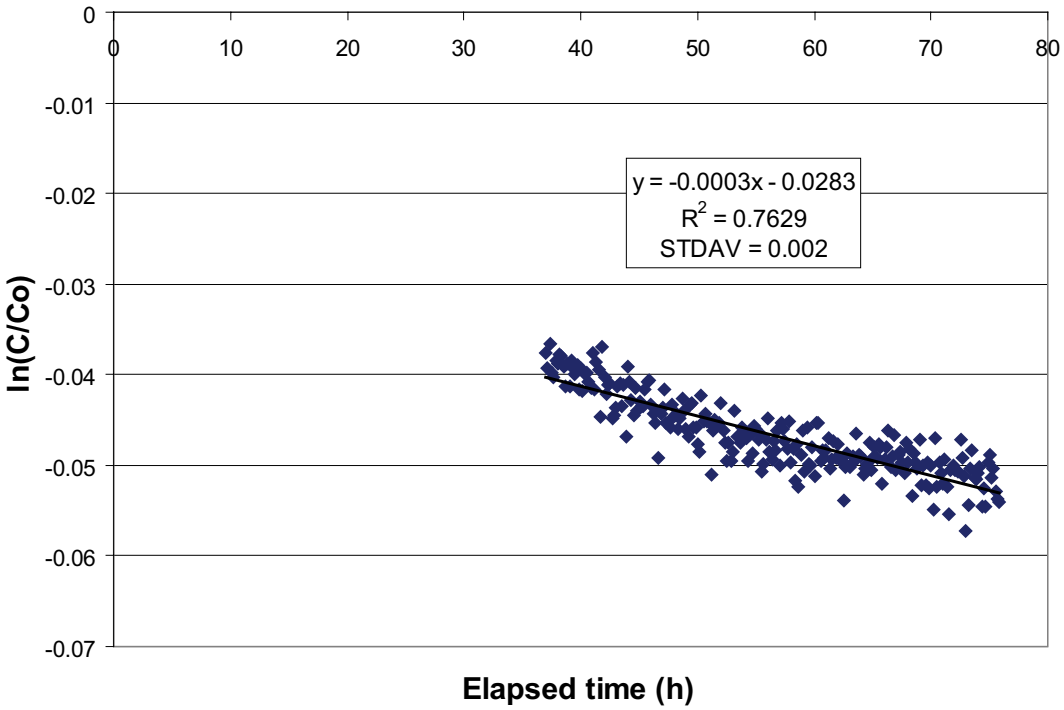


| Part of dilution curve (h) | V (ml) | ln(C/Co)/t | Q (ml/h) | Q (ml/min) | Q (m3/s) | R2-value |
|---|---|---|---|---|---|---|
| 37 - 75 | 3268 | -0.0003 | 0.98 | 0.016 | 2.72E-10 | 0.7629 |

| Part of dilution curve (h) | K (m/s) | Q (m3/s) | A (m2) | v(m/s) | I |
|---|---|---|---|---|---|
| 37 - 75 | 1.78E-09 | 2.72E-10 | 0.7700 | 3.54E-10 | 0.198 |

# Appendix C

## BIPS logging KFM04A

### BIPS logging in KFM04A

Adjusted depth range: 415.425–425.467 m

Black number = Recorded depth

Red number = Adjusted depth

Azimuth: 45

Scale: 1/25

Inclination: –60

Aspected ratio: 175%